Adaptive Visual Servoing in Uncalibrated Environments

Wang Hesheng

A Thesis Submitted in Partial Fulfilment of the

Requirements for the Degree of

Master of Philosophy

in

Automation and Computer-Aided Engineering

June 2004

Abstract

Visual servoing is a promising method to control dynamic systems using the information provided by visual sensors and has received extensive attention in recent years. Many existing methods work based on an assumption that the parameters of the vision system are accurately calibrated, while the calibration process is tedious. Furthermore, most of the controllers are designed using the kinematics relationship only, without any consideration of dynamics effect of robots, so that they are not suitable for high performance and fast visual servoing tasks.

Aiming at solving those two problems simultaneously, this thesis addresses dynamic control of robots with uncalibrated visual feedback. A novel method has been developed to regulate selected features to desired positions on the image plane by controlling the motion of the robot manipulator. We assume that the system is totally uncalibrated, i.e. both camera intrinsic parameters and the homogeneous transformation matrix between the robot frame and the vision frame are uncalibrated. Based on the important observation that the product of the image Jacobian matrix and the depth can be presented as a product of a known matrix and unknown parameters vector, an adaptive algorithm is developed to estimate the unknown

intrinsic and extrinsic parameters of the camera. The proposed controller adopts the simple PD plus the gravity compensation scheme with the estimated camera parameters. A new Lyapunov function is introduced to prove asymptotic convergence of the position errors on the image plane and convergence of the estimated parameters to the real ones up to a scale. The performance of the controller has been verified by computer simulations and experiments on a 3 DOF robot manipulator. The simulations and experiments results confirmed expected convergence and high performance of the proposed controller. This work contributes to the research of visual servoing and facilitates its applications greatly because with the proposed controller the tedious and difficult calibration task can be avoided.

简介

视觉伺服是一个用视觉传感器提供的信息来控制动态系统的有前途的方法, 近年来正受到广泛的重视。许多现存的方法假设视觉系统的参数被精确地标定，而标定的过程很繁琐。而且，大多数的控制器是基于运动学关系设计的而没有考虑机器人的动力学效应，以至于他们并不适合高性能和快速视觉伺服任务。

这篇论文陈述了用未标定的视觉反馈动态控制机器人，目的在于同时解决前面两个问题。我们研究了一个新的方法通过适当的控制机器手臂的运动来调节选择的特征点到期望的位置上。我们假设系统是完全非标定的，即相机的内部参数及机器人坐标系和视觉坐标系之间转换关系矩阵都未标定。 通过观察，我们注意到视觉 Jacobian 矩阵和深度的乘积可以表示为一个已知矩阵和为之参数的乘积，我们设计了一个自适应控制器，它可以求出包括相机内部和外部参数。提出的控制器采取了简单的比例积分加重力补偿的方案，控制器中含有求出的相机参数。我们引进了一个新的 Lyapunov 方程，可以证明图像平面的位置误差渐近收敛并且参数误差趋近真实值,但和真实值有一个比例系数。通过一个三自由度机械手臂的仿真和实验，这个控制器的特性被核实。仿真和实验结果证实了提出的控制器的期望收敛性和高性能。 因为这个控制器可以避免麻烦困难的标定工作，这个工作为视觉伺服的研究做出了贡献并且极大地推动了它的应用。

Acknowledgement

I am deeply indebted to my supervisor, Liu Yun-Hui, for his constant and generous advice, encouragement, and support. Many of the key ideas in this thesis arose in conversations with him, and this work would have been impossible without his help.

Thanks are also given to my colleagues in the Robot Control Lab for their support in many aspects of the research. I would like to thank specially Dr. Wai Keung Fung for discussing concepts and Mr. K. K. Lam for his help in the experimentation.

Finally, I wish to thank my parents for their unconditional support over many years.

Contents

List of Figures

List of Tables

Chapter 1

Introduction

1.1 Visual Servoing

Visual servoing is a robot control technique that uses vision in feedback control loops. Though the first systems date back to the late 1970s and early 1980s, it is not until the middle 1990s that there is a sharp increase in publications and working systems, due to the availability of fast and affordable vision processing systems.

Visual servoing is an approach to control robots based on visual perception, involving the use of cameras to position robots relative to the environment as required by the task. Hence, the general idea behind visual servoing is to derive the relationship between the robot and the sensor space and estimate a velocity screw associated with the robot frame needed to minimize the specified error.

Visual servoing involved many different research areas including robot modeling (geometry, kinematics, dynamics), real–time systems, control theory, systems (sensor) integration, computer vision (image processing, structure–from–motion, camera

calibration). There are many different ways of classifying the reported results: based on sensor configuration, number of cameras used, generated motion command (2D, 3D), scene interpretation, underlying vision algorithms.

People had used feedback control for a long time, but it is until recently, the development of the computer and especially the digital camera made the visual servo control available and affordable. Since its debut in the 1980's, it has attracted increasing interest from both industry and academia. The approaches from disciplines such as robotics, high-speed image processing, and real-time control had addressed the issue from different facets. The richness of the data that can be derived from vision, as well as the inherent need of endures to observe visual images, motivates the use of vision in controlling robot systems. Combining this with the complexity of the systems to be controlled makes visual servoing a uniquely challenging but exciting research area.

Just as the term implies, there are two essential foundations of the visual servo control: vision and control. Early research in this area had achieved moderate success by separating the visual control problem into these two constitutive components, study them individually, then simply combine the effort together by transferring the information from the vision to the control. This approach is often called "look-then-move". However, it will only be successful where either the speed of the system or its internal dynamics do not play a significant role.

Recently, researchers started to integrate the vision and control efforts by merging vision and control through image-based control. In this approach, the computation of the control inputs (and generally the specification of the goal states) is performed directly in the image plane. When this is possible, it allows one to bypass the computation of pose (i.e., position and orientation), and generally reduces the errors that may be introduced when transitioning between the visual image and robot pose spaces.

In terms of the design of visual servoing systems, there are two major issues that have to be considered: i) the choice of control law to provide the feedback for the control loop, ii) camera-robot configuration. We will touch upon the two issues briefly in the following section.

Visual servo robot control overcomes the difficulties of uncertain models and unknown environments. In the literature, there are two types of visual servo controllers: Position-based visual servo control and image-based visual servo control. They use the relative position and orientation of the target object with respect to the camera frame, to form the six elements pose vector. Also, in both classes of methods, object feature points are mapped onto the camera image plane, and measurements of these points are used for robot control [1].

1.1.1 Position-based Visual Servoing

In a position-based control system, the control error function is computed in the 3D Cartesian space. The pose of the target with respect to the camera, which describes its 3D position and 3D orientation, is estimated from image features corresponding to the perspective projection of the target in the image.

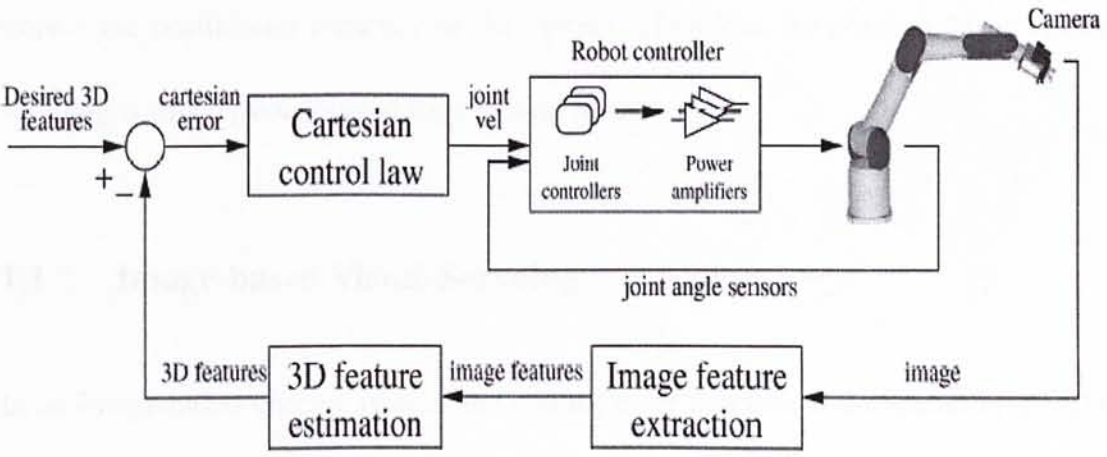

Figure 1.1: Position-based visual servoing.

The main advantage of position-based visual servoing is that it controls the camera trajectory in the Cartesian space, which allows it to easily combine the visual positioning task with obstacles avoidance and singularities avoidance [2]. Position-based methods for visual servoing seem to be the most generic approach to the problems, as they support arbitrary relative position with respect to the object.

The major disadvantage of position-based methods is that the 3D positions of the feature points must be estimated. In position-based visual servoing, feedback is computed using estimated quantities that are a function of the system calibration parameters. Hence, in some situations, position-based control can become extremely sensitive to calibration error. Particularly in stereo systems, small errors in computing the orientation of the cameras can lead to reconstruction errors that impact the positioning accuracy of the system. Therefore, the position-based visual servoing is usually not adopted for servoing tasks.

1.1.2 Image-based Visual Servoing

In an image-based control system, the control error function is computed in the 2D image plane. The general approach used in the image-based visual control methods is to control the robot motion in order to move the image plane features to desired positions. This usually involves the calculation of an image Jacobian or a composite Jacobian, the product of the image and robot Jacobian. A composite Jacobian relates differential changes in joint angles to differential changes in image features. The image-based control has the input command described directly in the feature space; it is then easy to generate the input trajectory by video-aid, computer-aided design. Image-based visual servoing control is considered to be very robust with respect to

camera and robot calibration errors. Coarse calibration only affects the rate of convergence of the control law in the sense that a longer time is needed to reach the desired position.

One disadvantage of image-based methods compared to position-based methods is the presence of singularities in the feature mapping function, which reflect themselves as unstable points in the inverse Jacobian control law.

The estimation of the image Jacobian requires knowledge of the camera intrinsic and extrinsic parameters. Extrinsic parameters also represent a rigid mapping between the scene or some reference frame and the camera frame. If one camera is used during the servoing process, the depth information needed to update the image Jacobian is lost. Therefore, many of the existing systems usually rely on a constant Jacobian that is computed for the desired camera/end–effector pose. This is one of the drawbacks of this approach, since the convergence is ensured only around the desired position. This problem may be solved by adaptive estimation of the depth.

In general, image-based visual servoing is known to be robust not only with respect to camera but also to robot calibration errors. Therefore, most of visual servo controllers are image-based. Also this method normally assumes that the range of the object is known. Adaptive control methods are normally employed.

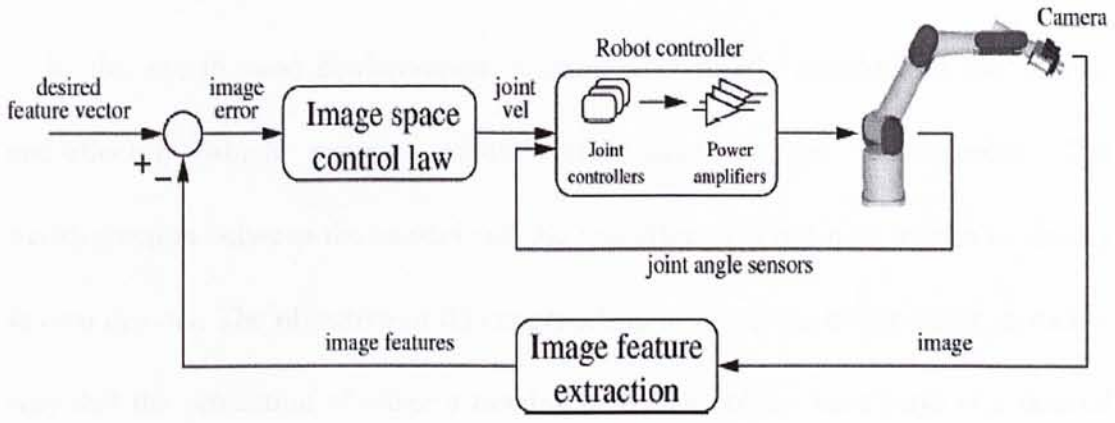

Figure 1.2: Image-based visual servoing.

1.1.3 Camera Configurations

Visual feedback is an important approach to improve the control performance of robot manipulators [3]. This robot control strategy, so-called visual servoing, based on monocular configuration, can be classified in two approaches: eye-and-hand system and eye-in-hand system.

In eye-and-hand robotic systems, a camera is fixed in the world-coordinate frame and targets are mounted on a robot end-effector. Camera is used as a global sensor and it capture images of both the robot and its environment. The objective of this approach is to make the robot move in such a way that its end-effector reaches a

desired object.

In the eye-in-hand configuration, a camera is rigidly attached to the robot's end-effector, which supplies visual information of the environment. The transformation between the camera and the end-effector coordinate frames is usually known *apriori*. The objective of this approach is to move the manipulator in such a way that the projection of either a moving or a static object be always at a desired location in the image captured by the camera [4].

Systems using a monocular camera usually adopt some form of model based visual techniques to facilitate the estimation of the depth between the camera and the object. If the camera is used as a global sensor, a geometric model of the object is commonly used to retrieve the full pose of the object. On the other hand, in the eye-in-hand configuration, feature and window based tracking techniques are more common. A single camera minimizes the processing time needed to extract visual information. However, the loss of depth information limits the types of servoing operations that can be performed as well as complicating the control design.

For either choice of camera configuration, camera calibration must be performed in order to execution visual servo tasks.

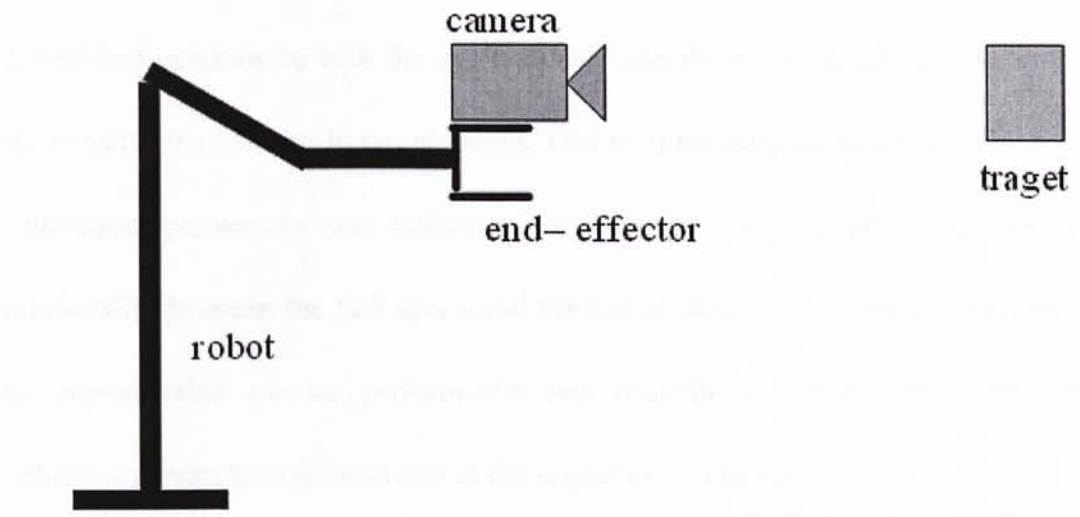

Figure 1.3: Eye-in-hand camera configuration.

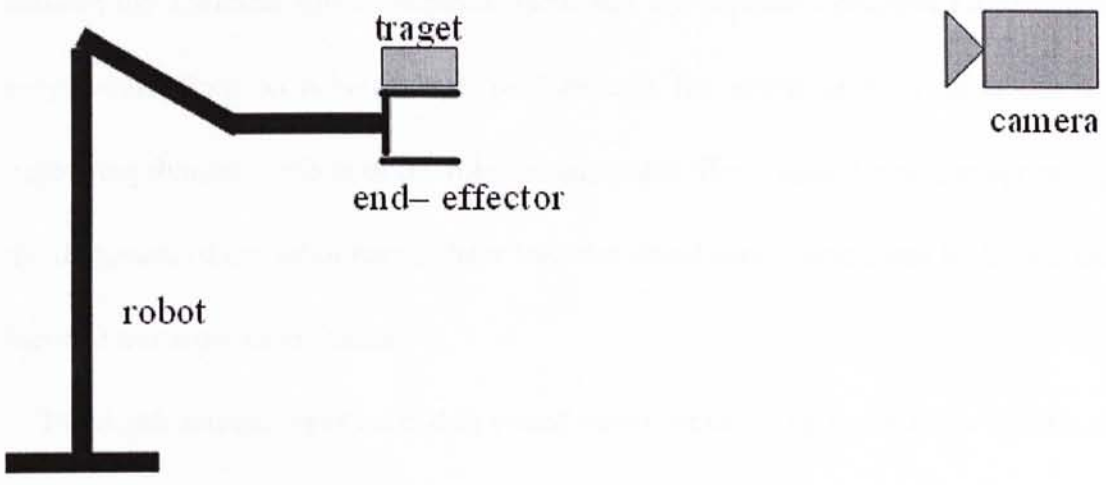

Figure 1.4: Eye-and-hand camera configuration

1.2 Problem Definitions

A problem common to both the eye-and-hand and the eye-in-hand configuration is the need for the cameras to be calibrated. That is, if the intrinsic and extrinsic camera calibration parameters are unknown, or slowly change over time, then the relationship between the task-space and the image-space will be erroneous, leading to unpredictable robotic performance and instability. Hence, estimating these unknown parameters online is one of the important works in this thesis.

Another issue that has impacted the development of robust vision-based controllers is that few visual servo controllers have been proposed that take into account the nonlinear robot dynamics. However, the methods considered kinematics only would limit to achieve high performance for visual servo system due to neglecting dynamic effects of the robot manipulator. Here, considering incorporating the dynamics of the robot manipulator into the visual servo controllers is the second focus of our work in the thesis.

The depth estimation is needed in visual servo control. The depth observability is the vital problem in the depth estimation, which determines the success of the estimation. The unknown depths were in the image Jacobian matrix of the image-based control, which make projection matrix nonlinear. The depth is usually changes with robot manipulator movement, which increases the difficulty in visual

servoing. How to compensate the nonlinear terms in Jacobian matrix and estimate depth is also a work addressed by us in the thesis.

1.3 Related Work

Previous approaches to visual servoing assumed known and accurate measures of camera parameters, camera positioning with respect to manipulator positioning, target depth [5]. Recently there has been a significant amount of research activity on the uncalibrated image-based visual servoing control. Some of the previous work on visual servoing assumes that the parameters can be identified in an off-line process. A control scheme with off-line parameter identification is not robust for disturbance change of parameters, and unknown environments. To overcome such defects, some on-line parameter identification schemes are proposed. Papanikolopoulos et al [6] proposed an algorithm based on on-line estimation for the relative distance of the target with respect to the camera. Hosada et al. [7] employed the Broyden updating formula to estimate the image Jacobian. Yoshimi et al. [8] utilized a simple geometric property to estimate image Jacobian. Feddema et al. [9] modeled the system making use of ARMAX model and estimated the coefficients of the model. Papanikolopoulos et al. [10] estimated the depth related parameters. However, The initial research efforts in this area did not take the dynamics of the robot into account.

Motivated by the desire to take into account uncalibrated camera effects and the dynamics of the robot, several researchers have recently designed visual servo controllers that ensure the convergence of the image error for the setpoint regulation problem. For example, Kelly et al [11], develop a regulation controller for the eye-in-hand problem, provided exact knowledge of the robot gravitational term is available and that depth information is known. In [12], Kelly and Marquez designed a setpoint controller for the eye-and-hand problem that compensated for unknown intrinsic camera parameters, provided perfect knowledge of the camera orientation was available. In [13], Kelly redesigned the setpoint controller take into account uncertainties associated with the camera orientation; however, the controller required that the difference between the estimated and actual camera orientation be restricted to the interval (–90◦, 90◦). In [14], Zergeroglu et al. proposed a uniformly ultimately bounded (UUB) setpoint controller for the eye-in-hand configuration provided the camera orientation is within a certain range. In [15], Maruyama and Fujita proposed position setpoint controllers for the eye-in-hand configuration; however, the proposed controllers required exact knowledge of the camera orientation and assumed equal camera scaling factors.

In addition to the setpoint regulation problem, several results have also been proposed for the tracking problem. For example, in [14], Zergeroglu et al. proposed a UUB position tracking controller with back stepping technique under the assumption

that the image plane is parallel to motion plane of the robot manipulator. In [16], Bishop and Spong developed an adaptive visual servo position tracking control scheme for the eye-and-hand configuration that compensated for camera calibration errors in the feedback loop; however, convergence of the position tracking error required that the desired position trajectory be persistently exciting. In [17], Kelly et al. proposed a two-loop visual servoing control system, which consists of an inner joint velocity servo controller and an image-based feedback outer loop; however, exact model knowledge of the robot dynamics and a calibrated camera are required, and the difference between the estimated and actual camera orientation is restricted to the interval (–90°, 90°). In [18], Target tracking by model independent visual servo control is achieved by augmenting quasi-Newton trust region control with target prediction. They use Broyden's Jacobian update approach. Recently, in [19], Zergeroglu et al. considers the problem of position tracking control of planar robot manipulators via visual servoing in the presence of parametric uncertainty associated with the robot mechanical dynamics and/or the camera system. Note that for the camera-in-hand configuration, due to the relative velocity problem associated with the eye-in-hand configuration, camera calibration is further necessitated by the need to relate the velocities between the camera and the image-space objects.

Until now, the unknown depths were in the feature Jacobian matrix of the feature-based control; the depth estimation is needed in visual servo control. In some

cases, the exact value of depth may not be necessary for the stability of the visual servo control scheme. The depth is still important information for handling the object. The depth observability is the vital problem in the depth estimation, which determines the success of the estimation. Although there have been several methods proposed for the depth estimation, depth estimate remain a difficult task in uncalibrated visual servoing. A practical way to obtain the depth is by using external sensors as ultrasound or additional cameras in the so-called binocular stereo approach [11]. Some other schemes use images obtained from different (more than two) points in the called active monocular stereo approach, and least-square techniques [20]. However, these methods estimate depth off-line. For achieving high performance visual servoing, some approaches have been used to estimate depth online; however, most researchers consider planar robot manipulator move parallel with image plane [13] [21] [22]. In these cases, depth is considered as constant parameters. They avoid estimate time-varying depth, the most difficult task. Also these are idea condition and not general case. Ezio Malis et al [23] [24] propose a new approach to vision based robot control, called 2-1/2-D visual servoing. However, they did not consider robot dynamics. Chien Chern Cheah et al [25] [26], propose simple feedback control laws for setpoint control without exact knowledge of kinematics, Jacobian matrix, and dynamics under sufficient conditions. In [27] [28] [29] [30] [31], they present adaptive methods to estimate depth on-line, however, they assume that the intrinsic

parameter are known. Other typical estimator in this system is the extended Kalman filter [3] [32] [33], also they only consider depth as unknown.

As seen the above, most of visual servoing methods do not consider totally uncalibrated case, and few approach estimates all these parameters on-line and considers the full robot dynamics.

1.4 Contribution of This Work

The purpose of this paper is to design a new image-based visual servoing system in totally uncalibrated environments. We point out our attention to one typical application of visual servoing: eye-and-hand system. The task is divided into two steps. In the first off-line learning step, the end-effector is moved to its desired position. The image of the target corresponding to this position is acquired and the extracted desired features are stored. In the second on-line step, the end-effector is controlled so that the current features reach their desired position in the image.

We assume the system is totally uncalibrated, i.e. both camera intrinsic parameters and the homogeneous transformation matrix between the robot frame and the vision frame are uncalibrated. The full dynamics of manipulator is also taken into account. Following are the summarized contributions of this thesis:

(1) We developed an adaptive law to estimate the unknown parameters including

the camera intrinsic parameters and the homogeneous transformation matrix between the robot frame and the vision frame. The estimate parameters asymptotically approach to the actual ones up to a scale.

(2) We designed an image-based visual regulation controller for an eye-and-hand system, when the camera intrinsic parameters and the homogeneous transformation matrix between the robot frame and the vision frame are not calibrated. It is proved with Lyapunov approach that the controller guarantees asymptotic convergence of the feature points errors on the image plane corresponding to the motion of the robot manipulator.

(3) The performance of the controller has been demonstrated by computer simulations and experiments on a 3 DOF robot manipulator. Simulations and experiments results verified the performance of asymptotic convergence of the proposed controller.

1.5 Organization of This Thesis

The paper is organized as follows. In Chapter 2, system model issues include the basics of robot kinematics; dynamics and camera models are addressed. In Chapter 3, uncalibrated image-based visual servoing controller is discussed. Simulation results are addressed in Chapter 4. Experimental results are addressed in Chapter 5. Finally,

in Chapter 6, the work done in this thesis is concluded and future work is outlined.

Chapter 2

System Modeling

In visual servoing, a camera produces the input signal, which must ultimately be transformed into joint commands to the robot controller. It is possible to divide this into three coordinate systems: the camera frame, Cartesian robot frame, and joint space. The derivation of the transformations from the camera to Cartesian frame and from Cartesian to joint space will be presented.

2.1 The Coordinates Frames

Figure 2.1 shows a set up of the system for eye-and-hand system. There are a robot manipulator and a fixed camera. There are 3 coordinates,

$\sum_B$: the robot base frame.

$\sum_E$: the end-effector coordinate frame.

$\sum_C$: the vision frame. ${}^{C}T_{B} = \begin{bmatrix} R & T \\ 0 & 1 \end{bmatrix}$ is the homogeneous transformation matrix of

$\sum_B$ with respect to $\sum_C$. The parameter R is the rotation matrix and T is a translation vector.

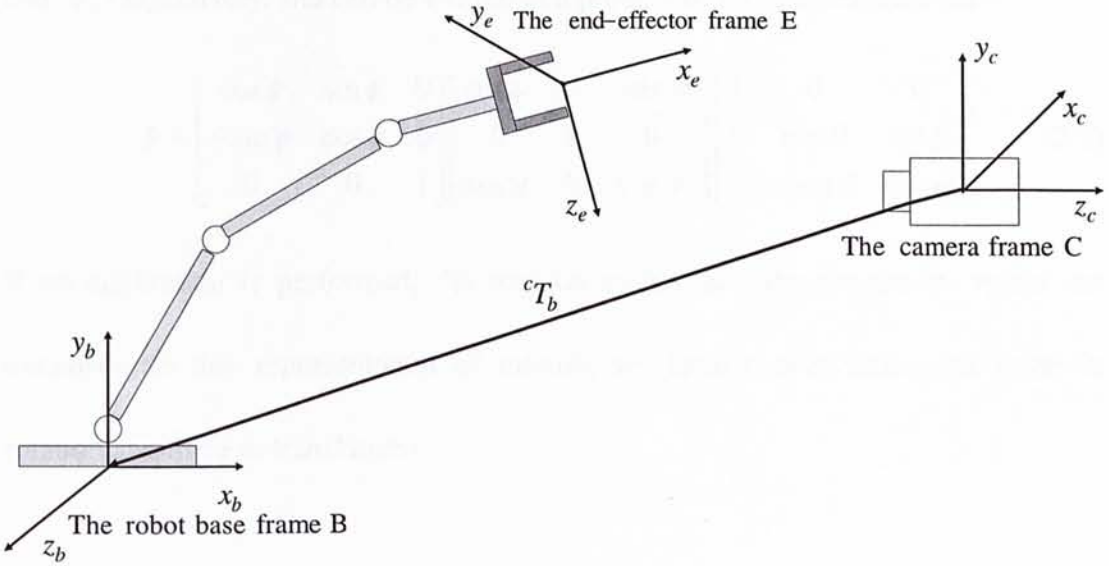

Figure 2.1: The coordinate frames.

Suppose that $\sum_C$ is the camera frame with the origin being at the optical center of the camera and Z-axis perpendicular to the image plane. Then we have

$$\begin{bmatrix} {}^cx \\ {}^cy \\ {}^cz \end{bmatrix} = {}^cR_b \begin{bmatrix} {}^bx \\ {}^by \\ {}^bz \end{bmatrix} + T \tag{2.1}$$

where $[{}^cx, {}^cy, {}^cz]^T$ and $[{}^bx, {}^by, {}^bz]^T$ are the coordinates of a point p in the camera frame and the base frame of the robot, respectively. Rotation can be specified in a

number of equivalent ways. For example, rotation can be around an axis passing through the origin of the coordinate system with an angle. Alternatively, R can be specified as three successive rotations around the x-, y-, and z-axis, by angles θ, ψ, and ϕ, respectively, and can be written as a product of these three rotations

$$R = \begin{bmatrix} \cos\phi & \sin\phi & 0 \\ -\sin\phi & \cos\phi & 0 \\ 0 & 0 & 1 \end{bmatrix} \begin{bmatrix} \cos\psi & 0 & -\sin\psi \\ 0 & 1 & 0 \\ \sin\psi & 0 & \cos\psi \end{bmatrix} \begin{bmatrix} 1 & 0 & 0 \\ 0 & \cos\theta & \sin\theta \\ 0 & -\sin\theta & \cos\theta \end{bmatrix} \tag{2.2}$$

If no calibration is performed, the rotation matrix and the translation vector are unknown. In this representation of motion, we have twelve unknowns (nine in rotation and three in translation).

2.2 The System Kinematics

Kinematics is the science of motion that refers to its geometrical and time-bade properties. It deals with position variables and their derivatives (with respect to time and other variables). We consider a class of robot manipulator with all revolute joints. From the forward Kinematics:

$$^{B}x_{E} = f(q) \tag{2.3}$$

where $^{B}x_{E} = [^{b}x_{e1}, ^{b}x_{e2}, ^{b}x_{e3}, ^{b}x_{e4}, ^{b}x_{e5}, ^{b}x_{e6}]^{T}$ present the position and orientation of the end-effector with respect to the base frame. The first three components of $^{B}x_{E}$ denote the position vector, and the other three components represent the orientation.

q is the joint angles of the robot manipulator. $f(q)$ is generally a nonlinear transformation describing the relation between the joint space and task space and is determined by the forward kinematics equation of the manipulator.

The task-space velocity ${}^{B}\dot{x}_{E}$ is related to joint-space velocity $\dot{q}$ as

$$ {}^{B}\dot{x}_{E} = J(q)\dot{q} \tag{2.4}$$

where ${}^{B}\dot{x}_{E}$ is the velocity of the end-effector with respect to the base frame. $\dot{q}$ is the joint velocities and *J(q)* is the robot Jacobian matrix of the robot manipulator. The velocity of end-effector with respect to the vision frame:

$$ {}^{c}\dot{x} = \begin{bmatrix} {}^{c}R_{b} & 0 \\ 0 & {}^{c}R_{b} \end{bmatrix} J(q)\dot{q} = AJ(q)\dot{q} \tag{2.5}$$

Then

$$ \dot{q} = J^{-1}(q)A^{T}\dot{x} \tag{2.6}$$

where assume *J(q)* is square and nonsingular.

2.3 The System Dynamics

Dynamics is the science of how motion is caused by forces and torques. In the absence of friction or other disturbances, the dynamics of a serial *n*-link rigid robot manipulator can be written as:

$$H(q)\ddot{q}+C(q,\dot{q})\dot{q}+G(q)=\tau \tag{2.7}$$

Where

q: $n\times 1$ vector of joint coordinates.

$H(q)$: $n\times n$ symmetric and positive definite inertia matrix.

$C(q,\dot{q})\dot{q}$: $n\times 1$ vector of centripetal and Coriolis torques.

$G(q)$: $n\times 1$ vector of gravity force.

τ: $n\times 1$ vector of applied joint torques.

Note that the frictional term has not been involved in this equation.

The visual servo control algorithms in the following chapters are based on some important properties of dynamic equation of manipulator in equation (2.7). They are follows:

Property 1 The inertia matrix $H(q)$ is symmetric and positive definite, and satisfies the following inequalities for $\forall \zeta \in R^2$

$$m_1\|\zeta\|^2 \le \zeta^T H(q)\zeta \le m_2(q)\|\zeta\|^2 \tag{2.8}$$

where m_1 is a positive constant, $m_2(x)$ is a positive function, and $\|\cdot\|$ denotes the standard Euclidean norm.

Property 2 The matrix $N(q,\dot{q})=\dot{H}(q)-2C(q,\dot{q})$ is skew-symmetric for a particular choice of $C(q,\dot{q})$ (which is always possible), i.e.,

$$z^T N(q,\dot{q})z=0 \tag{2.9}$$

for any $n \times 1$ vector z.

Property 3 The left-hand side of equation (2.7) can be linearly parameterized as shown below

$$H(q)\ddot{q} + C(q,\dot{q})\dot{q} + G(q) = W_1(q,\dot{q},\ddot{q})\Phi \tag{2.10}$$

where $\Phi \in R^m$ contains the constant system parameters and the regression matrix $W_1(\cdot) \in R^{2\times m}$ contains known functions dependent on the signals q, $\dot{q}$ and $\ddot{q}$.

Property 4 The gravity vector $G(q)$ verifies

$$\|G(q)\| \leq g_0 \tag{2.11}$$

for some bounded constant $g_0 > 0$

2.4 The Camera Model

In order to perform visual servo control, the relationships between the robot frame and the camera image plane must be known. In general, these relationships are defined in terms of a set of projection equations that define how points in the workspace project onto the camera image plane via the imaging geometry of the camera.

In the robotics and computer vision communities, CCD cameras are described using a range of models. In the following, we briefly present the most commonly

used models; as a common denominator, they do not model the camera at a physical level, but on an idealized, geometrical one. The distance between image plane and optical center, f, corresponds to the focal length of the camera.

The most common approximation to the real optics of a camera is the so-called pinhole camera model. The projection of a point onto the image plane is modeled as a central projection through the optical center, i.e. the center of the lens. This is illustrated in Figure 2.3. Note, that for a more intuitive visualization the image plane is depicted in front of the optical center instead of behind; therefore, the image does not appear inverted, as it would be in reality.

Pinhole cameral models include perspective projection and affine projection. When a scene's relief is small compared with the overall distance separating it from the camera observing it, affine projection models can be used to approximate the imaging process. These include the orthographic, parallel, weak-perspective and paraperspective projection.

We first describe three projection models that have been widely used to model the image formation process: perspective projection, weak-perspective projection and paraperspepective projection. Figure 2.2 show the three widely used projection models. Let c denote the optical center of this camera, and let P_0 denote a scene reference point; the weak-perspective projection of a scene point P_i is constructed in two steps: P_i is first projected orthographically onto a point of object plane parallel to

the image plane; perspective projection is then used to map this point onto the image point P_i^w. The paraperspective model takes into account both the distortions associated with a reference point that is off the optical axis of the camera and possible variations in depth: a scene point P_i is first projected parallel with the projection line of the reference point P_0 onto the object plane; perspective projection is then used to map this point onto the image point P_i^p.

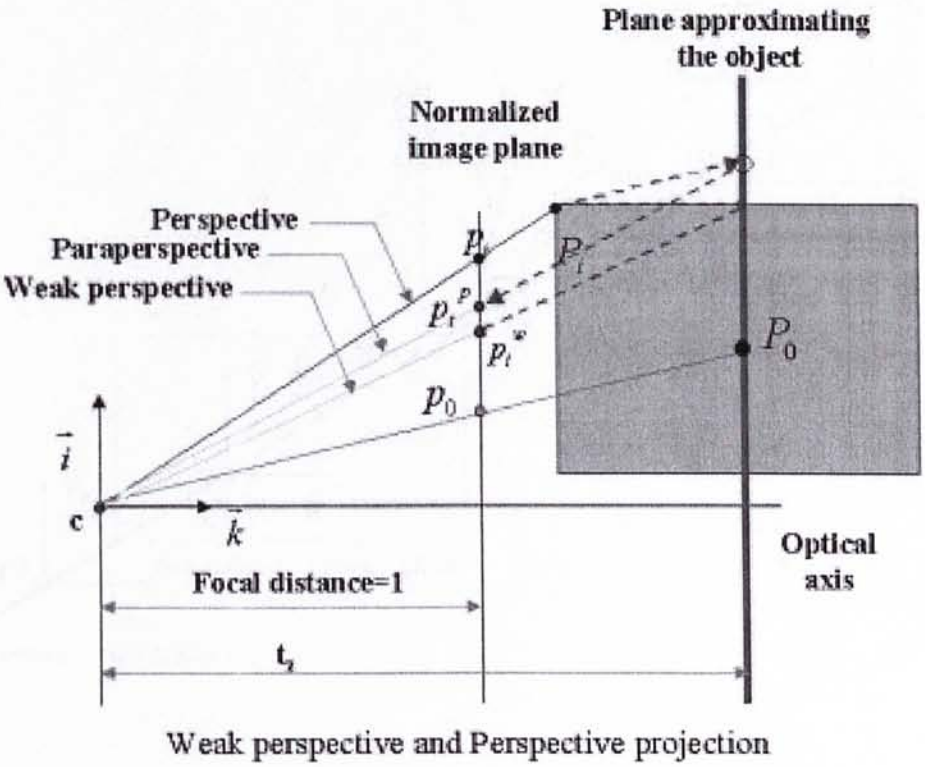

Figure 2.2: Three widely used projection models

We assume that the projective geometry of the camera is modeled by perspective

projection. As a mathematical tool, projective geometry has become very popular in the computer vision community, mostly because the perspective projection of the world onto an image plane can be modeled and analyzed very elegantly. Since that no explicit 3D information is to be extracted form an image, depth information is lost during projection.

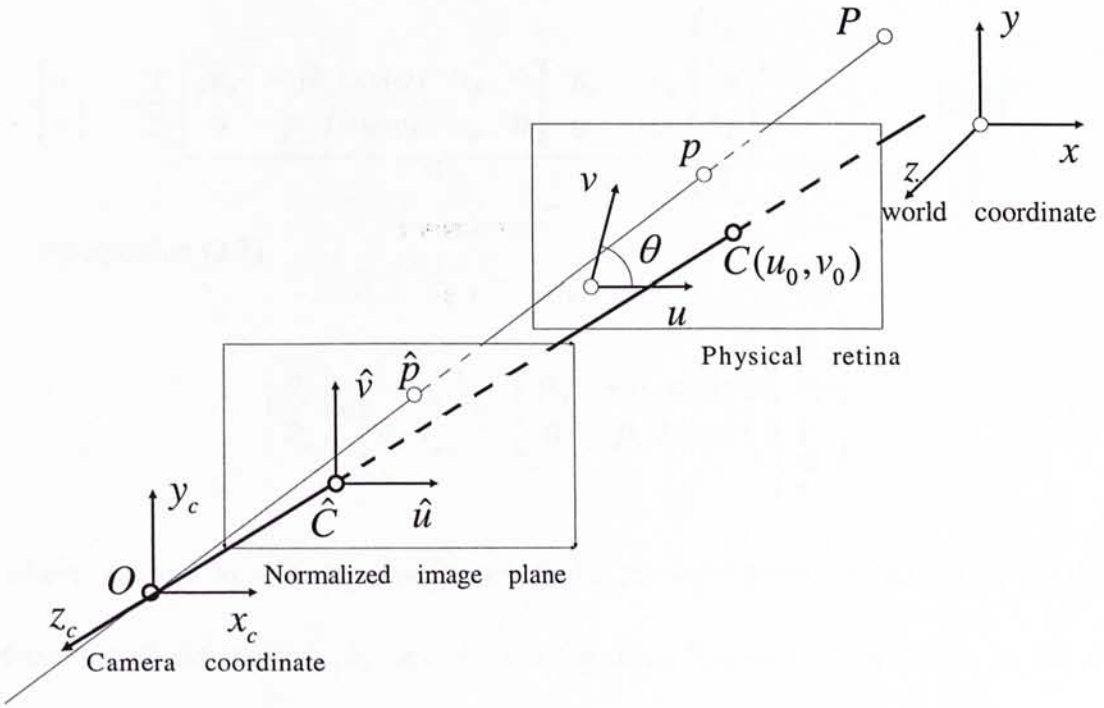

Figure 2.3: Perspective Projection

The image of the scene on the CCD is digitalized and transferred to the computer

memory and displayed on the computer screen. We define the two dimensional computer image (screen) coordinate frame $\sum_D = \{u, v\}$. The origin of $\sum_D$ is attached at the lower left corner of the computer screen while the axes u and v are selected parallel to the screen rows and columns respectively.

A point on the end-effector is ${}^cX = [X_c, Y_c, Z_c]^T$, whose coordinates are expressed with respect to the camera frame projects onto a point on the computer image plane as

$$\begin{bmatrix} u \\ v \end{bmatrix} = -\frac{1}{Z_c} \underbrace{\begin{bmatrix} fk_u & -fk_u \cos(\varphi) & u_0 & 0 \\ 0 & fk_v / \sin(\varphi) & v_0 & 0 \end{bmatrix} \begin{bmatrix} {}^cR_b & {}^cp_b \\ 0 & 1 \end{bmatrix}}_{M} \begin{bmatrix} {}^bx \\ {}^by \\ {}^bz \\ 1 \end{bmatrix} \tag{213}$$

By equation (2.1)

$$\begin{bmatrix} B_u \\ B_v \end{bmatrix} = \begin{bmatrix} u - u_o \\ v - v_o \end{bmatrix} = -\begin{bmatrix} fk_u & -fk_u \cos(\varphi) \\ 0 & fk_v / \sin(\varphi) \end{bmatrix} \begin{bmatrix} \frac{X_c}{Z_c} \\ \frac{Y_c}{Z_c} \end{bmatrix} \tag{2.12}$$

where u_0 and v_0 are the coordinates of the principal point (in pixels), f is the focal length (in meters), k_u and k_v are the magnifications, respectively, in the $\vec{u}$ and $\vec{v}$ direction (in pixels/meters), and φ is the angle between these axes. In general, the camera internal parameters are not perfectly known. For simplicity, we define $a_u = fk_u$, $a_v = fk_v / \sin(\varphi)$ and $\gamma = -fk_u \cos(\varphi)$. Usually, we can assume the image axial perpendicularly with each other. Then $\gamma = 0$ So (2.12) becomes

$$\begin{bmatrix} B_u \\ B_v \end{bmatrix} = -\begin{bmatrix} a_u & 0 \\ 0 & a_v \end{bmatrix} \begin{bmatrix} \frac{X_c}{Z_c} \\ \frac{Y_c}{Z_c} \end{bmatrix} \tag{2.13}$$

This model is so-called the imaging model. The time derivative of equation (2.13) yields

$$\begin{bmatrix} \dot{u} \\ \dot{v} \end{bmatrix} = -\begin{bmatrix} a_u & 0 \\ 0 & a_v \end{bmatrix} \begin{bmatrix} \frac{\dot{X}_c Z_c - X_c \dot{Z}_c}{Z_c^2} \\ \frac{\dot{Y}_c Z_c - Y_c \dot{Z}_c}{Z_c^2} \end{bmatrix} = -\begin{bmatrix} a_u & 0 \\ 0 & a_v \end{bmatrix} \begin{bmatrix} \frac{1}{Z_c} & 0 & -\frac{X_c}{Z_c^2} \\ 0 & \frac{1}{Z_c} & -\frac{Y_c}{Z_c^2} \end{bmatrix} \begin{bmatrix} \dot{X}_c \\ \dot{Y}_c \\ \dot{Z}_c \end{bmatrix} \tag{2.14}$$

Following, we discuss two camera configurations.

2.4.1 Eye-in-hand System.

Any displacement of a rigid object can be described by a rotation about an axis through the origin and a translation [34]. Let us assume that the camera moves in a static environment with a translational velocity T and with an angular velocity Ω with respect to the camera coordinate frame. The velocity of point P with respect to $\sum_V$ is:

$$\dot{P} = -\Omega \times P - T \tag{2.15}$$

Substituting the equation (2.15) into equation (2.14), we can obtain

$$\begin{bmatrix}\dot{u}\\ \dot{v}\end{bmatrix}=\begin{bmatrix}a_u & 0\\ 0 & a_v\end{bmatrix}\begin{bmatrix}\frac{1}{Z_c} & 0 & -\frac{X_c}{Z_c^2} & -\frac{X_cY_c}{Z_c^2} & 1+\frac{X_c^2}{Z_c^2} & -\frac{Y_c}{Z_c}\\ 0 & \frac{1}{Z_c} & -\frac{Y_c}{Z_c^2} & -(1+\frac{Y_c^2}{Z_c^2}) & \frac{X_cY_c}{Z_c^2} & \frac{X_c}{Z_c}\end{bmatrix}\begin{bmatrix}T_x\\ T_y\\ T_z\\ \omega_x\\ \omega_y\\ \omega_z\end{bmatrix} \tag{2.16}$$

We change the camera velocity respect to camera frame to the end-effector velocity with respect to the base frame.

$$\begin{bmatrix}T_x\\ T_y\\ T_z\\ \omega_x\\ \omega_y\\ \omega_z\end{bmatrix}=\begin{bmatrix}{}^cR_b & 0\\ 0 & {}^cR_b\end{bmatrix}\begin{bmatrix}I & -k({}^bR_e\,{}^er)\\ 0 & I\end{bmatrix}\begin{bmatrix}T_e\\ \Omega_e\end{bmatrix} \tag{2.17}$$

Substituting the equation (2.17) into equation (2.14), we can obtain

$$\begin{bmatrix}\dot{u}\\ \dot{v}\end{bmatrix} = \begin{bmatrix}a_u & 0\\ 0 & a_v\end{bmatrix}\begin{bmatrix}\frac{1}{Z_c} & 0 & -\frac{X_c}{Z_c^2} & -\frac{X_cY_c}{Z_c^2} & 1+\frac{X_c^2}{Z_c^2} & -\frac{Y_c}{Z_c}\\ 0 & \frac{1}{Z_c} & -\frac{Y_c}{Z_c^2} & -(1+\frac{Y_c^2}{Z_c^2}) & \frac{X_cY_c}{Z_c^2} & \frac{X_c}{Z_c}\end{bmatrix} \tag{2.18}$$
$$\times\begin{bmatrix}{}^cR_e & 0\\ 0 & {}^cR_e\end{bmatrix}\begin{bmatrix}{}^eR_b & 0\\ 0 & {}^eR_b\end{bmatrix}\begin{bmatrix}I & -k({}^bR_e\,{}^er)\\ 0 & I\end{bmatrix}\begin{bmatrix}T_e\\ \Omega_e\end{bmatrix}$$

Continually, we may rewrite equation (2.18) in such a form as follows

$$\begin{bmatrix} \dot{u} \\ \dot{v} \end{bmatrix} = -\begin{bmatrix} -\frac{a_u}{Z_c} & 0 & -\frac{B_u}{Z_c} & -\frac{B_u B_v}{a_v} & -a_u - \frac{B_u^2}{a_u} & -\frac{a_u B_v}{a_v} \\ 0 & -\frac{a_v}{Z_c} & -\frac{B_v}{Z_c} & a_v + \frac{B_v^2}{a_v} & -\frac{B_u B_v}{a_u} & \frac{B_u a_v}{a_u} \end{bmatrix} \times \begin{bmatrix} {}^c R_e & 0 \\ 0 & {}^c R_e \end{bmatrix} \begin{bmatrix} {}^e R_b & 0 \\ 0 & {}^e R_b \end{bmatrix} \begin{bmatrix} I & -k({}^b R_e\, {}^e r) \\ 0 & I \end{bmatrix} \begin{bmatrix} T_e \\ \Omega_e \end{bmatrix} \tag{2.19}$$

In order to guarantee the object that can be observed fully, three or more feature points attached on the object rigidly are required for the visual servo control to be solvable. Here we have

$$\begin{bmatrix} \dot{u}_1 \\ \dot{v}_1 \\ \dot{u}_2 \\ \dot{v}_2 \\ \dot{u}_3 \\ \dot{v}_3 \\ \vdots \end{bmatrix} = J_s \begin{bmatrix} T_x \\ T_y \\ T_z \\ \omega_x \\ \omega_y \\ \omega_z \end{bmatrix} \tag{2.20}$$

where

$$J_s = -\begin{bmatrix} -\frac{a_u}{Z_c} & 0 & -\frac{B_{u1}}{Z_c} & -\frac{B_{u1}B_{v1}}{a_v} & -a_u - \frac{B_{u1}^2}{a_u} & -\frac{a_u B_{v1}}{a_v} \\ 0 & -\frac{a_v}{Z_c} & -\frac{B_{v1}}{Z_c} & a_v + \frac{B_{v1}^2}{a_v} & -\frac{B_{u1}B_{v1}}{a_u} & \frac{B_{u1}a_v}{a_u} \\ -\frac{a_u}{Z_c} & 0 & -\frac{B_{u2}}{Z_c} & -\frac{B_{u2}B_{v2}}{a_v} & -a_u - \frac{B_{u2}^2}{a_u} & -\frac{a_u B_{v2}}{a_v} \\ 0 & -\frac{a_v}{Z_c} & -\frac{B_{v2}}{Z_c} & a_v + \frac{B_{v2}^2}{a_v} & -\frac{B_{u2}B_{v2}}{a_u} & \frac{B_{u2}a_v}{a_u} \\ -\frac{a_u}{Z_c} & 0 & -\frac{B_{u3}}{Z_c} & -\frac{B_{u3}B_{v3}}{a_v} & -a_u - \frac{B_{u3}^2}{a_u} & -\frac{a_u B_{v3}}{a_v} \\ 0 & -\frac{a_v}{Z_c} & -\frac{B_{v3}}{Z_c} & a_v + \frac{B_{v3}^2}{a_v} & -\frac{B_{u3}B_{v3}}{a_u} & \frac{B_{u3}a_v}{a_u} \end{bmatrix} \tag{2.21}$$

Where J_s is the so-called image Jacobian matrix and $J_s \in \Re^{2n\times 6}, n \geq 3$ is number of the feature points. Here we use 3 pair of feature points. To combine equation (2.20) and equation (2.4), we obtain

$$\dot{\xi} = J_s {}^c\dot{X} = J_s J(q)\dot{q} \tag{2.22}$$

As we can see, the Jiacobian matrix J_s consists of the camera parameters such as focal length, aspect ratio, distortion coefficients, and the kinematic parameters such as translation and rotation between the camera coordinate and the robot base coordinate.

Equation (2.22) relates Feature space to Cartesian space. This mapping involves nonlinearities due to radial lens distortion, perspectivity, and quantization issues between the camera and the end-effector frame. The robot Jacobian is a highly coupled and nonlinear function of joint angles and robot dimensions. Some researchers have proposed using adaptive schemes to find a matrix of constant coefficients to approximate the total image Jacobian. It is possible to find certain configurations of the robot where the total image Jacobian changes slowly, but this severely restricts the robot workspace.

Assume J_s is nonsingular, then we have

$$\dot{q} = J^+(q) J_s^+ \dot{\xi} \tag{2.23}$$

where $J^+(q)$ mean pseudoinverse of matrix $J(q)$.

2.4.2 Eye-and-hand System

Let us assume that the end-effector moves in a static environment with a translational velocity T_E and with an angular velocity Ω with respect to the base frame. Suppose there is a point P in the end-effector, where $r(x, y, z)$ is the coordinate respect to center of the end-effector we assume known. The velocity of point with respect to $\sum_b$ is:

$$^b\dot{P} = \Omega \times {}^bR_e\, {}^e r + T_e \tag{2.24}$$

Substituting equation (2.24) into equation (2.14), we can obtain,

$$\begin{bmatrix} \dot{u} \\ \dot{v} \end{bmatrix} = -\frac{1}{Z_c}\begin{bmatrix} a_u & 0 & B_u \\ 0 & a_v & B_v \end{bmatrix}\begin{bmatrix} {}^c\dot{X} \\ {}^c\dot{Y} \\ {}^c\dot{Z} \end{bmatrix} = -\frac{1}{Z_c}\begin{bmatrix} a_u & 0 & B_u \\ 0 & a_v & B_v \end{bmatrix} {}^cR_b \begin{bmatrix} {}^b\dot{X} \\ {}^b\dot{Y} \\ {}^b\dot{Z} \end{bmatrix} \tag{2.25}$$

The motion of the image feature point as a function of the camera velocity is obtained by substituting equation (2.24) into equation (2.25),

$$\begin{bmatrix} \dot{u} \\ \dot{v} \end{bmatrix} = -\frac{1}{Z_c}\begin{bmatrix} a_u & 0 & B_u \\ 0 & a_v & B_v \end{bmatrix} {}^cR_b \begin{bmatrix} I & -k({}^bR_e\, {}^e r) \end{bmatrix}\begin{bmatrix} T_e \\ \Omega \end{bmatrix} = J_{s1}\begin{bmatrix} T_e \\ \Omega \end{bmatrix} \tag{2.26}$$

where k is a matrix operator and $k(x)$ with vector $x = [x_1 \quad x_2 \quad x_3]^T$ can be written as a matrix form

$$k(x)=\begin{bmatrix} 0 & -x_3 & x_2 \\ x_3 & 0 & -x_1 \\ -x_2 & x_1 & 0 \end{bmatrix} \tag{2.27}$$

we define

$$S_i=\frac{1}{Z_i}\begin{bmatrix} a_u & 0 & u_i-u_0 \\ 0 & a_v & v_i-v_0 \end{bmatrix}{}^{c}R_b k({}^{b}R_e\,{}^{e}r_i) \tag{2.28}$$

In order to guarantee that the end-effector motion can be observed fully, three or more feature points attached on the end-effector rigidly are required for the visual servo control to be solvable. The above imaging model can be extended to an object located in the robot workspace having n object features points. In this case, the feature image velocity $\dot{\xi}$ is redefined as

$$\begin{bmatrix} \dot{u}_1 \\ \dot{v}_1 \\ \dot{u}_2 \\ \dot{v}_2 \\ \dot{u}_3 \\ \dot{v}_3 \\ \vdots \end{bmatrix}=J_s\begin{bmatrix} T_e \\ \Omega \end{bmatrix} \tag{2.29}$$

where J_s is the so-called image Jacobian matrix which include unknown parameters such as intrinsic parameters, the rotation matrix between the robot base frame and the vision frame and the depth parameter. $J_s\in\Re^{2n\times 6}, n\geq 3$ is number of the feature points.

$$J_s = \begin{bmatrix} -\frac{1}{Z_1}\begin{bmatrix} a_u & 0 & u_1 - u_0 \\ 0 & a_v & v_1 - v_0 \end{bmatrix} & S_1 \\ -\frac{1}{Z_2}\begin{bmatrix} a_u & 0 & u_2 - u_0 \\ 0 & a_v & v_2 - v_0 \end{bmatrix} & S_2 \\ -\frac{1}{Z_3}\begin{bmatrix} a_u & 0 & u_3 - u_0 \\ 0 & a_v & v_3 - v_0 \end{bmatrix} & S_3 \\ \vdots & \vdots \end{bmatrix} \tag{2.30}$$

Here, we define another matrix called *nonscaled image Jacobian*.

$$J_a = J_s D(-Z)$$

It should be noted that the elements of the nonscaled image Jacobian are linear to the elements of the perspective projection matrix

Finally, by using equation (2.4) and (2.29) we can express $\dot{\xi}$ in terms of the robot joint velocity $\dot{q}$ as

$$\dot{\xi} = J_s {}^e\dot{X} = J_s J(q)\dot{q} \tag{2.31}$$

Assume J_s is nonsingular, then we have

$$\dot{q} = J^+(q) J_s^+ \dot{\xi} \tag{2.32}$$

where $J^+(q)$ mean pseudoinverse of matrix $J(q)$.

Chapter 3

Adaptive Image-based Visual Servoing

3.1 Controller Design

The visual servo control algorithms in this chapter are based on some theories used to analyze stability of the visual servoing systems proposed in this thesis. Refer to Appendix A for details.

The robot task is specified in the image plane in terms of image features corresponding to observable points rigidly attached to the robot manipulator end-effector. In the control problem formulation considered in this chapter, the position of the feature points of the object can only be measured through the camera. Thus, a direct knowledge of the desired joint position is not available. However, in this chapter, we consider a controller, which consists of directly using the image feature error supplied in the image coordinate frame.

Let $\xi_d = [u_d, v_d]^T$ be the desired position with respect to the computer image frame of the target image feature corresponding to the attached point. Hereafter,

$\xi_d = [u_d, v_d]^T$ will be referred as the desired image feature vector which is constant because the target was assumed to be stationary.

The control problem is to design a controller to compute the applied torques such way that the image feature $\xi = [u, v]^T$ corresponding to the point attached to the robot manipulator end-effector reaches the desired image feature $\xi_d = [u_d, v_d]^T$ of the point attached to the target position. This formulation can be equivalently stated as driving the robot manipulator end-effector in such a way that the corresponding image feature $\xi = [u, v]^T$ reaches a constant arbitrary point $\xi_d = [u_d, v_d]^T$ into the computer image frame.

The approach followed in this chapter was motivated by the transpose Jacobian control philosophy proposed in [35] [36]. We design control law for eye-and-hand system.

The control law of the proposed controller is given by

$$\tau = G(q) - K_v \dot{q} - K_p J^T(q) \left(\hat{J}_a^T - \frac{1}{2} \hat{J}_e^T \right) \Delta\xi \tag{3.1}$$

where K_p and K_v are the symmetric positive-definite proportional and derivative matrices which are chosen by the designer. A signal over a parameter means that is an estimated value of the actual parameter. $\Delta\xi = \xi - \xi_d$ is image error we can directly obtain from computer screen. $D(Z)$ is a $2n \times 2n$ diagonal matrix and $n \geq 3$ is the number of the feature points.

$$D(Z)=\begin{bmatrix} Z_1 & & & & & & \\ & Z_1 & & & & & \\ & & Z_2 & & & & \\ & & & Z_2 & & & \\ & & & & Z_3 & & \\ & & & & & Z_3 & \\ & & & & & & \ddots \end{bmatrix} \tag{3.2}$$

Then

$$J_s=\begin{bmatrix} \begin{bmatrix} 0 & 0 & u_1-u_{d1} \\ 0 & 0 & v_1-v_{d1} \end{bmatrix} & S_1' \\ \begin{bmatrix} 0 & 0 & u_2-u_{d2} \\ 0 & 0 & v_2-v_{d2} \end{bmatrix} & S_2' \\ \begin{bmatrix} 0 & 0 & u_3-u_{d3} \\ 0 & 0 & v_3-v_{d3} \end{bmatrix} & S_3' \\ \vdots & \vdots \end{bmatrix} \tag{3.3}$$

where (u_d, v_d) is the desired image point and

$$S_i'=\begin{bmatrix} 0 & 0 & u_i-u_{di} \\ 0 & 0 & v_i-v_{di} \end{bmatrix} {}^cR_b k({}^bR_e {}^e r_i) \tag{3.4}$$

Even if the exact Jacobian matrix is used in task-space control, the manipulator could stall at a singular posture or the control torques could also become very large when the desired position is close to singularity. Conventional ways of dealing with singularities usually keep the manipulator away from them at the inverse-kinematics level, or assuming that the robot operates in a subspace which excludes the singular points.

It is worth noticing that the controller uses directly the feature error vector $\Delta\xi$, which is the difference between the desired feature vector and the actual one expressed in the image coordinate frame. The controller also requires the measurement of the joint position and velocity, the estimated knowledge of the nonscaled image Jacobian matrix, and the gravitational torque vector $G(q)$. However, the solution of the inverse image and kinematics are obviated.

The closed-loop system is obtained by substituting the control Signal τ from the control law (3.1) into the robot dynamics (2.7)

$$H(q)\ddot{q} + C(q,\dot{q})\dot{q} = -K_v\dot{q} - K_p J^T(q)\left(\hat{J}_a^T - \frac{1}{2}\hat{J}_e^T\right)\Delta\xi \tag{3.5}$$

The robot dynamics include the unknown parameters, which must be determined on-line. In the same time, in order to guarantee that the image errors will go to zero when the joint velocities go to zero, the estimated image Jacobian matrix must be full rank. An effect way is to adaptive these parameters to actual ones up to a scale.

3.2 Estimation of The Parameters

Notice that the relationship between the camera coordinate and the robot base coordinate is

$$\begin{bmatrix} X \\ Y \\ Z \end{bmatrix} = {}^{c}R_{b}\begin{bmatrix} {}^{b}X \\ {}^{b}Y \\ {}^{b}Z \end{bmatrix} + {}^{c}T_{b} = \begin{bmatrix} {}^{c}R_{1b} & {}^{c}R_{2b} \\ {}^{c}R_{3b} & {}^{c}R_{4b} \end{bmatrix}\begin{bmatrix} {}^{b}X \\ {}^{b}Y \\ {}^{b}Z \end{bmatrix} + \begin{bmatrix} {}^{c}T_{1b} \\ {}^{c}T_{2b} \end{bmatrix} \tag{3.6}$$

Then

$$\begin{bmatrix} X \\ Y \end{bmatrix} = {}^{c}R_{1b}\begin{bmatrix} {}^{b}X \\ {}^{b}Y \end{bmatrix} + {}^{c}R_{2b}\,{}^{b}Z + {}^{c}T_{1b} \tag{3.7}$$

$$Z = {}^{c}R_{3b}\begin{bmatrix} {}^{b}X \\ {}^{b}Y \end{bmatrix} + {}^{c}R_{4b}\,{}^{b}Z + {}^{c}T_{2b} \tag{3.8}$$

Since the intrinsic parameters, the transformation matrix and the depth between the camera and the target are unknown when no calibration and no measurement are performed, then we propose

Proposition 1: *Arrange the m unknown elements of the product of the image Jacobian matrix and the depth matrix by a* $m\times 1$ *vector* θ. *For* 6×1 *vector* $\Delta\xi$, *the product of the matrix* $J_a^T - \frac{1}{2}J_e^T$ *with the vector can be represented in the following linear form*:

$$\left(J_a^T - \frac{1}{2}J_e^T\right)\Delta\xi = W(\Delta\xi,u,v,q)\theta \tag{3.9}$$

where $W(\Delta\xi,u,v,q)$ is a regressor matrix whose elements do not depend on the unknown parameters. Then

$$\left(J_a^T - \frac{1}{2}J_e^T\right)\Delta\xi - \left(\hat{J}_a^T - \frac{1}{2}\hat{J}_e^T\right)\Delta\xi = W(\Delta\xi,u,v,q)\Delta\theta \tag{3.10}$$

where $\Delta\theta = \theta - \hat{\theta}$ is the parameter errors, θ is real parameters. $\hat{\theta}$ is estimated ones.

Based on the projection equation (2.12), we consider the following approach for leading the estimated unknown parameters to tend to the actual ones up to a scale. Thus, an equation is defined

$$
\begin{aligned}
&-\hat{Z}_c\begin{bmatrix} u \\ v \end{bmatrix} - \left[\begin{bmatrix} \hat{a}_u & 0 \\ 0 & \hat{a}_v \end{bmatrix}\begin{bmatrix} {}^cX \\ {}^cY \end{bmatrix} - \hat{Z}_c\begin{bmatrix} \hat{u}_0 \\ \hat{v}_0 \end{bmatrix}\right] \\
&= -\hat{Z}_c\begin{bmatrix} u \\ v \end{bmatrix} - \left[\hat{H}\begin{bmatrix} {}^cX \\ {}^cY \end{bmatrix} - \hat{Z}_c\begin{bmatrix} \hat{u}_0 \\ \hat{v}_0 \end{bmatrix}\right] \\
&= \left[Z - \hat{Z}\right]\begin{bmatrix} u \\ v \end{bmatrix} - Z\begin{bmatrix} u \\ v \end{bmatrix} - \left[\hat{H}\left[{}^c\hat{R}_{1b}\begin{bmatrix} {}^bX \\ {}^bY \end{bmatrix} + {}^c\hat{R}_{2b}\,{}^bZ + {}^c\hat{T}_{1b}\right] - \hat{Z}_c\begin{bmatrix} \hat{u}_0 \\ \hat{v}_0 \end{bmatrix}\right] \\
&= \left[Z - \hat{Z}\right]\begin{bmatrix} u \\ v \end{bmatrix} + \left[H\,{}^cR_{1b} - \hat{H}\,{}^c\hat{R}_{1b}\right]\begin{bmatrix} {}^bX \\ {}^bY \end{bmatrix} + \left[H\,{}^cR_{2b} - \hat{H}\,{}^c\hat{R}_{2b}\right]{}^bZ \\
&\quad + \left[H\,{}^cT_{1b} - \hat{H}\,{}^c\hat{T}_{1b}\right] - \left[Z_c\begin{bmatrix} u_0 \\ v_0 \end{bmatrix} - \hat{Z}_c\begin{bmatrix} \hat{u}_0 \\ \hat{v}_0 \end{bmatrix}\right] \\
&= Y_1(u,v,q)\Delta\theta_1 + Y_2(q)\Delta\theta_2 + Y_3(q)\Delta\theta_3 + Y_4\Delta\theta_4 + Y_5(q)\Delta\theta_5 \\
&= Y_6(u,v,q)\Delta\theta
\end{aligned}
\tag{3.11}
$$

If n feature points are used, equation (3.11) can be extend to

$$-\begin{bmatrix} \hat{Z}_{1c}u_1 \\ \hat{Z}_{1c}v_1 \\ \hat{Z}_{2c}u_2 \\ \hat{Z}_{2c}v_2 \\ \hat{Z}_{3c}u_3 \\ \hat{Z}_{3c}v_3 \\ \vdots \end{bmatrix} - \left[\begin{bmatrix} \hat{H} & 0 & 0 & \cdots \\ 0 & \hat{H} & 0 & \cdots \\ 0 & 0 & \hat{H} & \cdots \end{bmatrix} \begin{bmatrix} {}^cX_1 \\ {}^cY_1 \\ {}^cX_2 \\ {}^cY_2 \\ {}^cX_3 \\ {}^cY_3 \\ \vdots \end{bmatrix} - \begin{bmatrix} \hat{Z}_{1c}\hat{u}_0 \\ \hat{Z}_{1c}\hat{v}_0 \\ \hat{Z}_{2c}\hat{u}_0 \\ \hat{Z}_{2c}\hat{v}_0 \\ \hat{Z}_{3c}\hat{u}_0 \\ \hat{Z}_{3c}\hat{v}_0 \\ \vdots \end{bmatrix} \right] = Y(u,v,q)\Delta\theta \qquad (3.12)$$

where $Y(u,v,q)$ is a $2n\times m$ regressor matrix without depending on any unknown parameters, where n presents number of the feature points, m presents number of the unknown parameters. In order to guarantee the parameters can be fully estimated, $n \geq m/2$ points are adopted.

Proposition 2: *If seven points are selected are they are not coplanar in the space, the equation*

$$Y(u,v,q)\Delta\theta = 0$$

is equivalent to that the parameters can be estimated up to a scale

$$\hat{\theta} = \lambda\theta$$

where λ is a scalar.

This result is well known in the computer vision, and the detailed proof can be referred to the book [38].

Remark 1: If $Y(u,v,q)\Delta\theta = 0$, in equation (3.12), we have $2n$ equations, which is not less than the number of the unknown parameters. Then we can conclude that all

these unknown parameters could be estimated. This will lead the estimated unknown parameters to tend to the actual ones up to a scale.

The following adaptive estimate method is proposed.

$$\Delta\dot{\theta}^T = -\frac{1}{K_1}\dot{q}^T K_p J^T(q) W(\Delta\xi, u, v, q) - \Delta\theta^T Y^T(u, v, q) K_2 Y(u, v, q) \qquad (3.13)$$

From the adaptive law,

$$\Delta\dot{\theta}^T K_1 \Delta\theta = -\dot{q}^T K_p J^T(q) W(\Delta\xi, u, v, q)\Delta\theta - \Delta\theta^T Y^T(u, v, q) K_1 K_2 Y(u, v, q)\Delta\theta \qquad (3.14)$$

3.3 Stability Analysis

This section analyzes the stability of the proposed controller and adaptive algorithm. Following is the main result of this thesis:

Theorem 1: The proposed controller in (3.1) and the adaptive estimated method (3.13) guarantee the image errors asymptotically converge to the region defined by the following equation

$$\left(\hat{J}_a - \frac{1}{2}\hat{J}_e\right)^T \Delta\xi = 0 \qquad (3.15)$$

Furthermore, the estimated parameters are convergent to the real values up to a scale.

Proof: We define the following function.

$$V = \frac{1}{2}\dot{q}^T H(q)\dot{q} + \frac{1}{2}\Delta\xi^T K_p D(-Z)\Delta\xi + \frac{1}{2}\Delta\theta^T K_1 \Delta\theta \tag{3.16}$$

where K_1 is a constant parameter and $K_1 > 0$.

Notice that $Z < 0$, then $D(-Z) > 0$. And also from robot dynamics Property 1, we can conclude that V is a positive definite function. Differentiating above (3.16) results in

$$\dot{V} = \dot{q}^T H(q)\ddot{q} + \frac{1}{2}\dot{q}^T \dot{H}(q)\dot{q} + \Delta\dot{\xi}^T K_p D(-Z)\Delta\xi + \frac{1}{2}\Delta\xi^T K_p D(-\dot{Z})\Delta\xi + \Delta\dot{\theta}^T K_1 \Delta\theta \tag{3.17}$$

From (2.31) and $\dot{\xi}_d = 0$, we obtain

$$K_p \dot{q}^T J^T(q) J_s^T D(-Z)\Delta\xi = \dot{\xi}^T K_p J_s^T D(-Z)\Delta\xi \tag{3.18}$$

and

$$\frac{1}{2}\Delta\xi^T K_p D(-\dot{Z})\Delta\xi = -\frac{1}{2}K_p \dot{Z}^T D(\Delta\xi)\Delta\xi = -\frac{1}{2}K_p \dot{q}^T J^T(q) J_e^T \Delta\xi \tag{3.19}$$

Substitute(3.18), (3.19) into above (3.17), then

$$\dot{V} = \dot{q}^T H(q)\ddot{q} + \frac{1}{2}\dot{q}^T \dot{H}(q)\dot{q} + K_p \dot{q}^T J^T(q) J_s^T D(-Z)\Delta\xi - \frac{1}{2}K_p \dot{q}^T J^T(q) J_e^T \Delta\xi + \Delta\dot{\theta}^T K_1 \Delta\theta \tag{3.20}$$

By regarding Property 2, we know

$$\dot{q}^T H(q)\ddot{q} + \frac{1}{2}\dot{q}^T \dot{H}(q)\dot{q} = \dot{q}^T H(q)\ddot{q} + \dot{q}^T C(q,\dot{q})\dot{q} \tag{3.21}$$

Substitute (3.5) into above (3.21), then

$$\dot{q}^T H(q)\ddot{q}+\frac{1}{2}\dot{q}^T \dot{H}(q)\dot{q}=-\dot{q}^T K_v\dot{q}-K_p\dot{q}^T J^T(q)\left(\hat{J}_a^T-\frac{1}{2}\hat{J}_e^T\right)\Delta\xi \tag{3.22}$$

Then we rewrite (3.20) as

$$\begin{aligned}\dot{V} \;=\; & -\dot{q}^T K_v\dot{q}-K_p\dot{q}^T J^T(q)\left(\hat{J}_a^T-\frac{1}{2}\hat{J}_e^T\right)\Delta\xi \\ & +K_p\dot{q}^T J^T(q)\left(J_a^T-\frac{1}{2}J_e^T\right)\Delta\xi+\Delta\dot{\theta}^T K_1\Delta\theta\end{aligned} \tag{3.23}$$

By using (3.10), we obtain

$$\dot{V}=-\dot{q}^T K_v\dot{q}+\dot{q}^T K_p J^T(q)W(\Delta\xi,u,v,q)\Delta\theta+\Delta\dot{\theta}^T K_1\Delta\theta \tag{3.24}$$

To make the above equation as a Lyapunov function, we use the proposed adaptive estimate method (3.13), then

$$\dot{V}=-\dot{q}^T K_v\dot{q}-\Delta\theta^T Y^T(u,v,q)K_1K_2Y(u,v,q)\Delta\theta \tag{3.25}$$

Then, $\dot{V}$ is nonpositive function. It states that V is a Lyapunov function. Since $\dot{V}$ is nonpositive function, V never increases. It means that $\dot{q}$, $\Delta\xi$ and $\Delta\theta$ are bounded. From LaSalle theorem, we can know $\lim\dot{q}\to 0$ and $\lim Y(u,v,q)\Delta\theta\to 0$, which implies that the estimated parameters will asymptotically converge to the actual ones up to a scale. Then from the robot dynamic (3.5), we can conclude that $\lim\left(\hat{J}_a-\frac{1}{2}\hat{J}_e\right)^T\Delta\xi\to 0$, where $\hat{J}_a$ is the estimated nonscaled image Jacobian matrix.

Since those feature points are on a rigid body, a stronger result can be obtained.

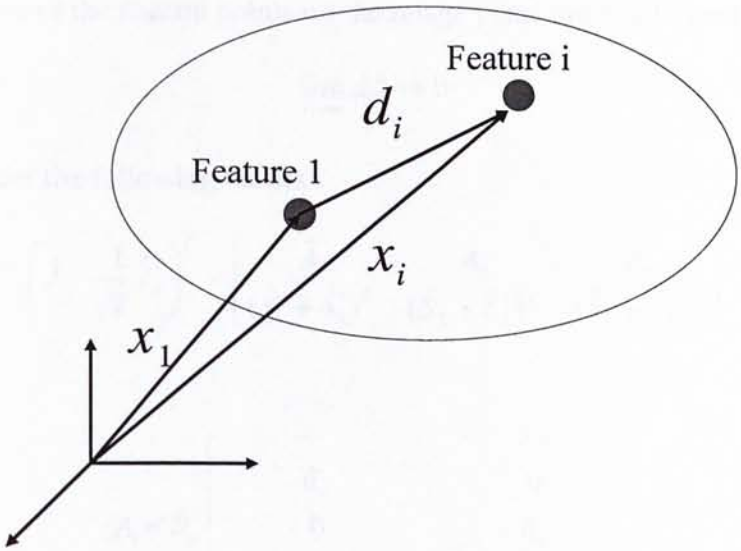

Figure 3.1: Feature points on a rigid body

Consider a feature point i and a reference feature, for example feature point 1, on a rigid body (figure 3.1). Their coordinates with respect to the robot base frame are related by

$$x_i = x_1 + R_r d_i \tag{3.26}$$

where R_r is the rotation matrix of the rigid body with respect to the robot base frame and d_i represents the vector from the feature point 1 to the feature point i, By the perspective projection transform,

$$\xi_i = -\frac{1}{{}^c z_i} M(x_1 + R_r d_i) = \frac{{}^c z_1}{{}^c z_i}\xi_1 - \frac{1}{{}^c z_i} M R_r d \tag{3.27}$$

Based on these analyses, we proposed:

Theorem 2: Under the control of the controller (3.1) and the adaptive rule (3.13), the

position errors of the feature points on the image plane are convergent to zero, i.e.

$$\lim_{t\to\infty} \Delta\xi \to 0$$

Proof: Consider the following matrix

$$\left(\hat{J}_a - \frac{1}{2}\hat{J}_e\right)^T = \begin{bmatrix} \hat{A}_1 & \hat{A}_2 & \hat{A}_3 \\ (\hat{S}_1 + \hat{S}_1')^T & (\hat{S}_2 + \hat{S}_2')^T & (\hat{S}_3 + \hat{S}_3')^T \end{bmatrix} \tag{3.28}$$

where

$$\hat{A}_i = {}^c\hat{R}_b^T \begin{bmatrix} \hat{a}_u & 0 \\ 0 & \hat{a}_v \\ \frac{1}{2}(u_i + u_{di}) - \hat{u}_0 & \frac{1}{2}(v_i + v_{di}) - \hat{v}_0 \end{bmatrix} \tag{3.29}$$

From equation (3.15), we can conclude

$$\left(\hat{J}_a - \frac{1}{2}\hat{J}_e\right)^T \Delta\xi = 0 \Rightarrow \sum_{i=1}^{3} \hat{A}_i \Delta\xi_i = 0 \tag{3.30}$$

By substituting the equation (3.27) into above equation (3.30),

$$\sum_{i=1}^{3} \frac{z_1}{z_i} \hat{A}_i \xi_i + \sum_{i=1}^{3} \hat{A}_i \left(\frac{1}{z_i}\hat{M}Rd_i - \xi_{di}\right) = 0 \tag{3.31}$$

Here we define,

$$\psi = \sum_{i=1}^{3} \frac{z_1}{z_i} \hat{A}_i \tag{3.32}$$

It is easy to note that $rank(\psi) = 2$. There exists only one solution for the image coordinates of the feature point 1 to satisfy equation (3.30), this implies that only one solution for all the feature points to satisfy equation (3.30) because of the one-to-one mappings of their positions defined by equation (3.27). On the other hand, the zero

position errors, i.e. $\Delta\xi_i = 0$ are obviously one solution of the equation (3.30). Therefore, all states must satisfy that $\Delta\xi_i = 0$. From LaSalle theorem, we can conclude the convergence of the position errors on the image plane of the feature points to zero.

Chapter 4

Simulation

In this chapter, we show the performance of the proposed image-based controller by simulations. We conducted the simulations on a 3 DOF manipulator, which neglect the last three joints of the Puma 560 manipulator. The physical parameters of Puma 560 are shown in the following figure.

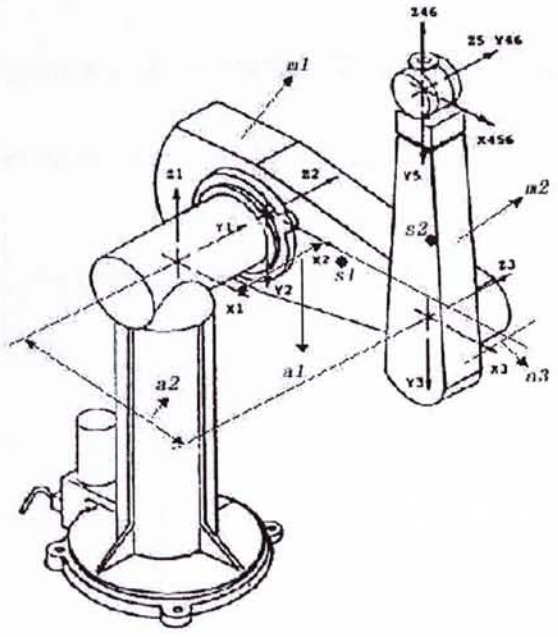

Figure 4.1: Robot manipulator

Where a1=243.5mm, a2=431.8mm, a3=93.4mm, m1=17.4kg, m2=4.8kg. In the following simulations, the three feature points are attached to the end-effector.

We first set initial position and record the image positions of these three points, then let the end-effector move to another position and record these image positions as the desired positions. In order to get comprehensive simulation results, two simulations are carried out.

4.1 Simulation I

In the first simulations, the initial image features coordinates are: $\xi_0 = (410.89 \quad 520.01 \quad 413.25 \quad 510.51 \quad 420.05 \quad 537.36)^T$ (pixels), and the desired ones are $\xi_d = (300.42 \quad 346.14 \quad 306.19 \quad 360.28 \quad 295.00 \quad 329.10)^T$ (pixels). The control gains are $K_p = 0.00002, K_v = 2, K_1 = 0.04$, $K_1 = 0.00012$. The rotation matrix between the robot frame and the vision frame is $R = \begin{bmatrix} 0 & 1 & 0 \\ 0.09 & 0 & 1 \\ 1 & 0 & 0.09 \end{bmatrix}$ the estimated one is $\hat{R} = \begin{bmatrix} 0 & 1 & 0 \\ 0.31 & 0 & 0.95 \\ 0.95 & 0 & -0.31 \end{bmatrix}$. Other parameters are in Table 4.1.

Parameters	**Values**	
	Real parameters	***Initial estimated parameters***
a_u (pixel)	800	900
a_v (pixel)	900	920
u_0 (pixel)	300	350
v_0 (pixel)	400	490
f (m)	0.01	0.02

Table 4.1: Parameters of simulation I

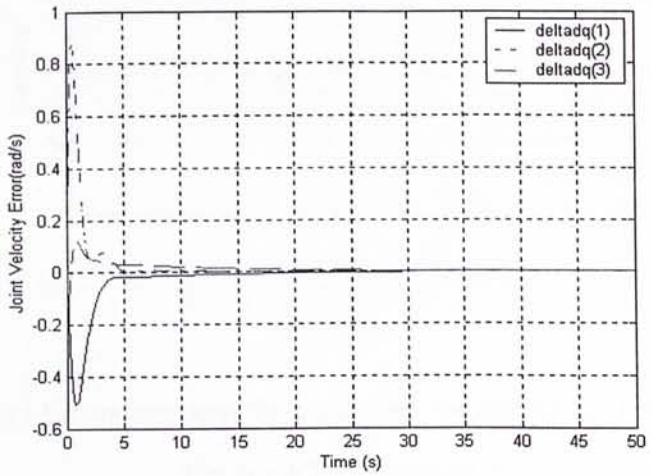

(a) Robot joint velocities;

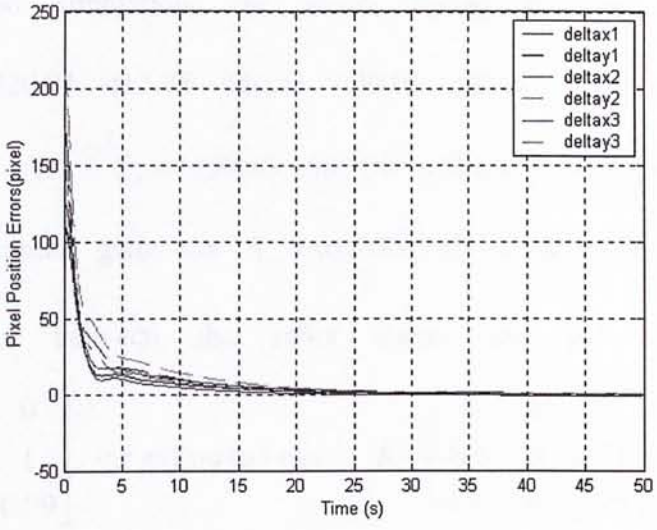

(b) Position errors of three screen image features;

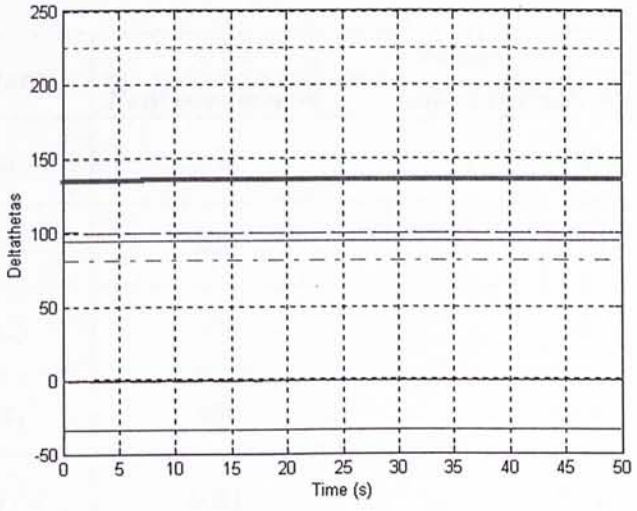

(c) Errors between the estimated and real parameters.

Figure 4.2: Simulation I

4.2 Simulation II

In the second simulation, the initial image features coordinates are: $\xi_0 = (410.89 \quad 520.01 \quad 413.25 \quad 510.51 \quad 420.05 \quad 537.36)^T$ (pixels), and the desired ones are $\xi_d = (459.46 \quad 582.06 \quad 452.69 \quad 577.73 \quad 476.67 \quad 590.52)^T$ (pixels). The control gains are $K_p = 0.00004$, $K_v = 1$, $K_1 = 0.4$. $K_2 = 0.0004$ The rotation matrix between the robot frame and the vision frame is $R = \begin{bmatrix} 0 & 1 & 0 \\ 0.09 & 0 & 1 \\ 1 & 0 & 0.09 \end{bmatrix}$, the estimated one is $\hat{R} = \begin{bmatrix} 0 & 1 & 0 \\ 0.5 & 0 & 0.87 \\ 0.87 & 0 & -0.5 \end{bmatrix}$. Other parameters are in Table 4.2.

Parameters	**Values**	
	Real parameters	***Initial estimated parameters***
a_u (pixel)	800	700
a_v (pixel)	900	920
u_0 (pixel)	300	450
v_0 (pixel)	400	490
f (m)	0.01	0.02

Table 4.2: Parameters of simulation II

As we can see from Figure 4.2 and Figure 4.3, the asymptotic convergence of the image errors is guaranteed. The sample time of simulation is 2ms.

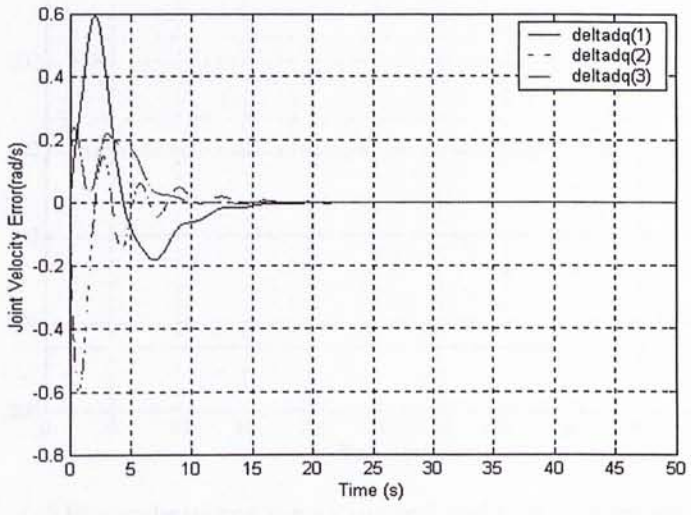

(a) Robot joint velocities;

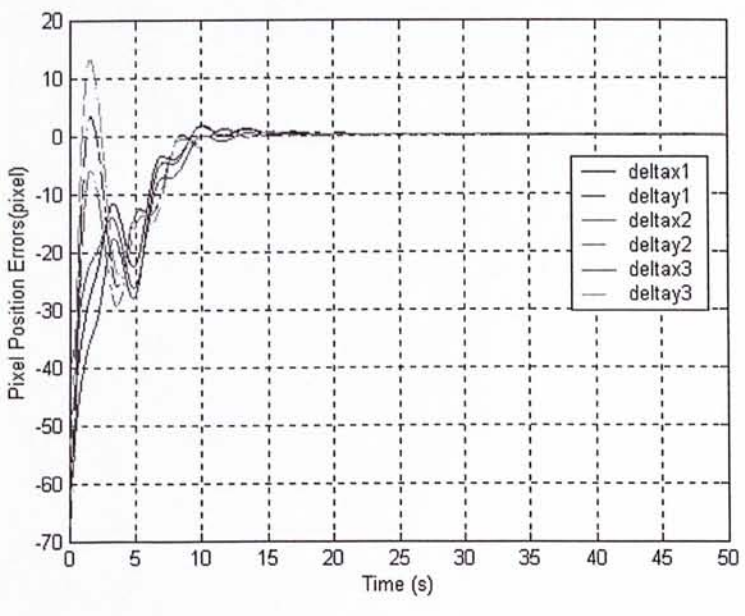

(b) Position errors of three screen image features;

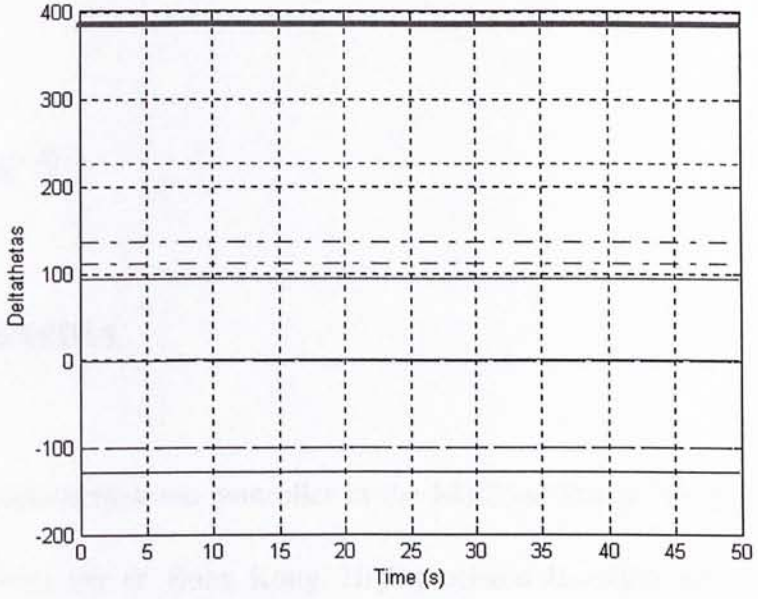

(c) Errors between the estimated and real parameters.

Figure 4.3: Simulation II

Chapter 5

Experiments

We have implemented the controller in the Modified Puma 560 Manipulator in the Chinese University of Hong Kong. High-precision Encoders are used to measure joint angles. The joint velocities are obtained by differentiating the joint angles. A control board mounted in a Pentium II computer, which provides an environment for the experimental execution, controls the robot manipulator. The proposed controller is programmed in C language.

We fixed a camera about 3 meters away from the robot manipulator. This camera is a high-resolution 2/3" format camera made by SONY company. It is model PULNiX TMC-76, which has a pixel array with $768(H)\times576(V)$. A frame processor MATROX PULSAR installed in a PC with Intel Pentium II CPU acquires the video signal. This PC processes the image and extracts the image features. The sample time of the experimental system is 120ms.

In order to evaluate the proposed image-based visual servo controller, we did several experiments. The control gains are chosen as: $K_p = 0.00002\,\mathrm{N\cdot m/pixels}$,

$K_v = 0.5\,\mathrm{N\cdot m\cdot s/deg}$, $K_1 = 0.5$. $K_2 = 0.000012$ The rotation matrix between the robot frame and the vision frame is $R = \begin{bmatrix} 0 & 1 & 0 \\ 0.09 & 0 & 1 \\ 1 & 0 & 0.09 \end{bmatrix}$ the estimated one is $\hat{R} = \begin{bmatrix} 0 & 1 & 0 \\ 0.31 & 0 & 0.95 \\ 0.95 & 0 & -0.31 \end{bmatrix}$. Other parameters are in Table 5.1.

Parameters	**Values**	
	Real parameters	***Initial estimated parameters***
a_u (pixel)	4763	4000
a_v (pixel)	4515	5000
u_0 (pixel)	550	400
v_0 (pixel)	300	400
f (m)	0.01	0.02

Table 5.1: Parameters of experiments

Figure 5.1 shows the 3 DOF robot manipulator used in experiments. This robot manipulator is developed by the Robot Control Lab in the Chinese University of Hong Kong. The patterns of feature points on the image are plotted in Figure 5.2. The three big dots in figure denote three desired image features on computer image plane. In Figure 5.3, we show a schematic of the system set up used for testing the

new visual controller. This system include a camera, a 3 DOF robot manipulator and a computer, they are connected with each other by several board installed in the computer.

In order to get comprehensive results, three experiments are carried out. The main difference between these three experiments is the initial position. The robot manipulator is set to different initial position and they should go to the same desired position. And the results are shown in Figure 5.4, 5.5 and 5.6.

Figure 5.4(a), 5.5(a) and 5.6(a) depict the three features position errors in image frame. The trajectories of the features on computer image plane are presented in Figure 5.4(b), 5.5(b) and 5.6(b). As shown in Figure 5.4, 5.5 and 5.6, the image feature points asymptotically converge to the desired ones. These experimental results verified the performance of the new controller.

The simulation and experimental results both verify asymptotic convergence of the proposed controller. However, the time period for simulation is about 2ms and for experiment is about 120ms, which make the experiment response relative slow compare to simulation one. Due to the uncertainty in camera intrinsic and extrinsic parameters in experiments, while these parameters are known accurate in simulations, the condition for simulation and experiments can not be set exactly the same. The object of simulations is to test the theory; the object of experiments is to test the controller in real environments.

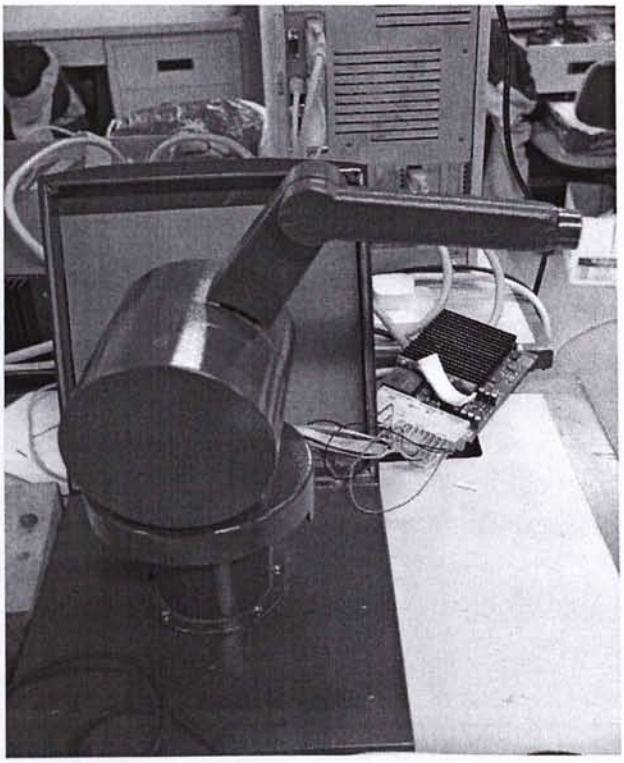

Figure 5.1: The 3 DOF robot manipulator used in experiments

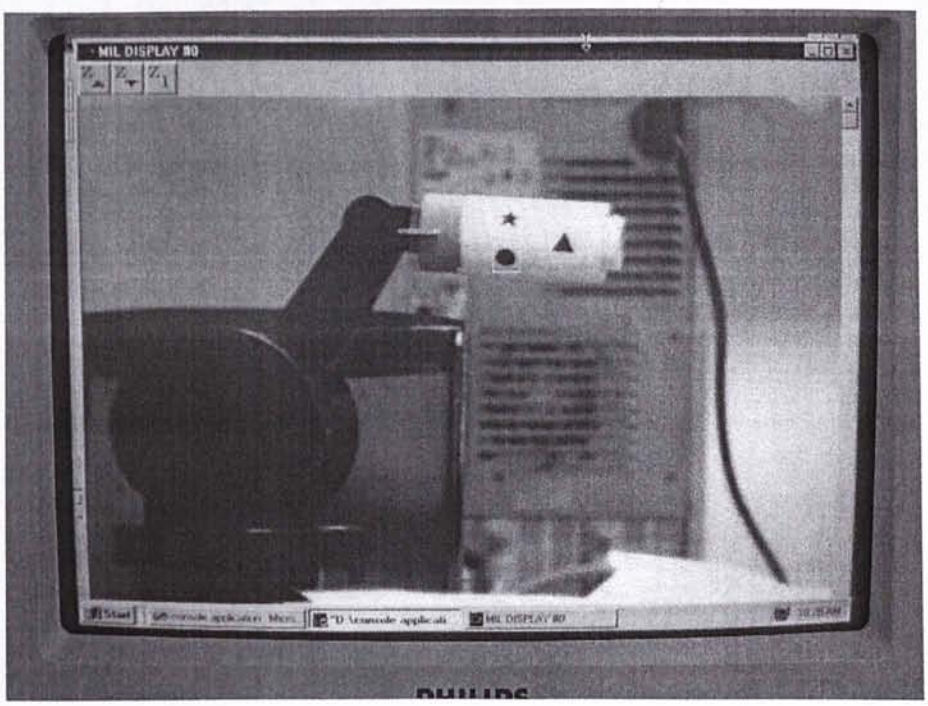

Figure 5.2: Patterns of the image feature points

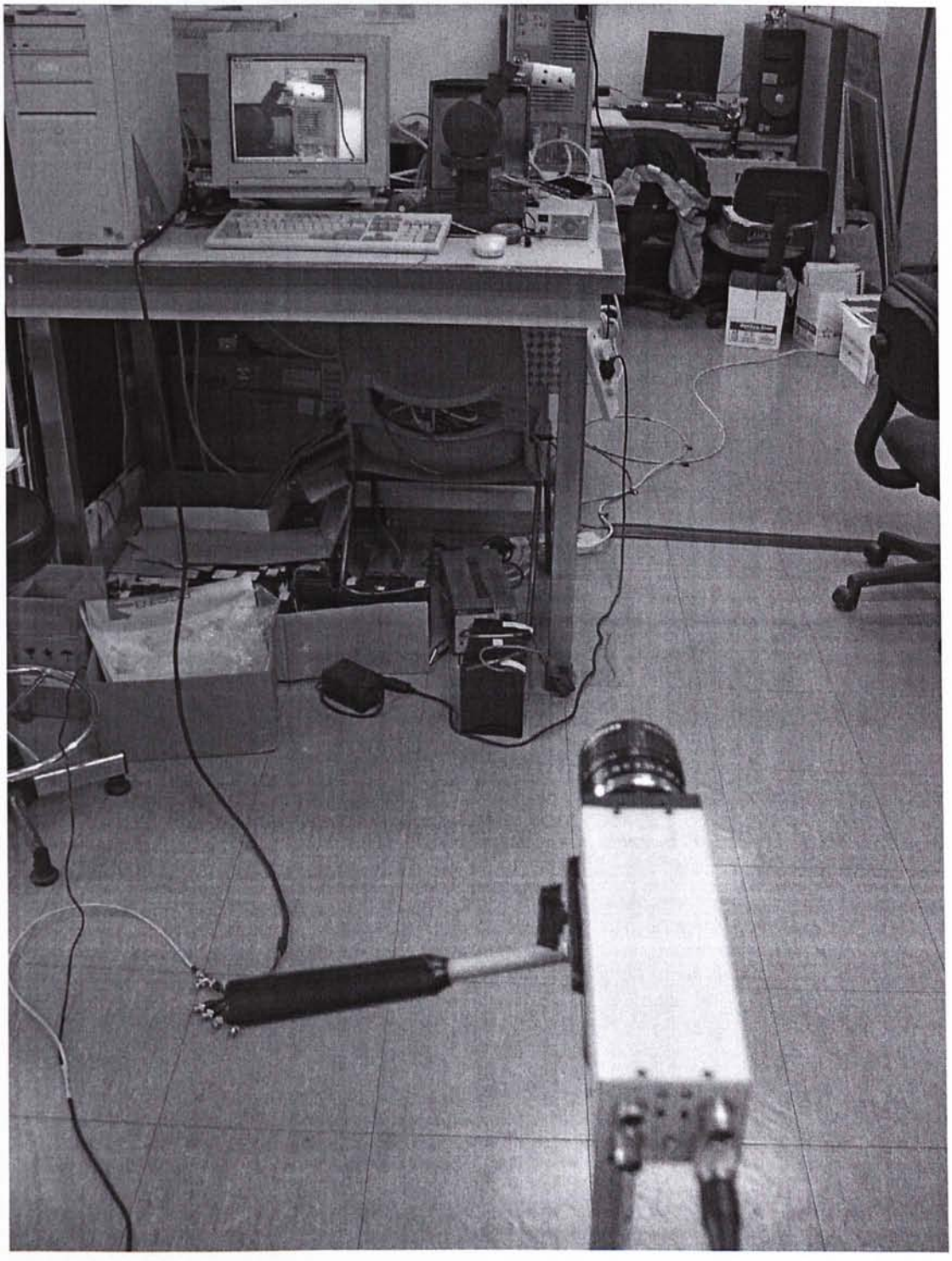

Figure 5.3: The experiment set up system

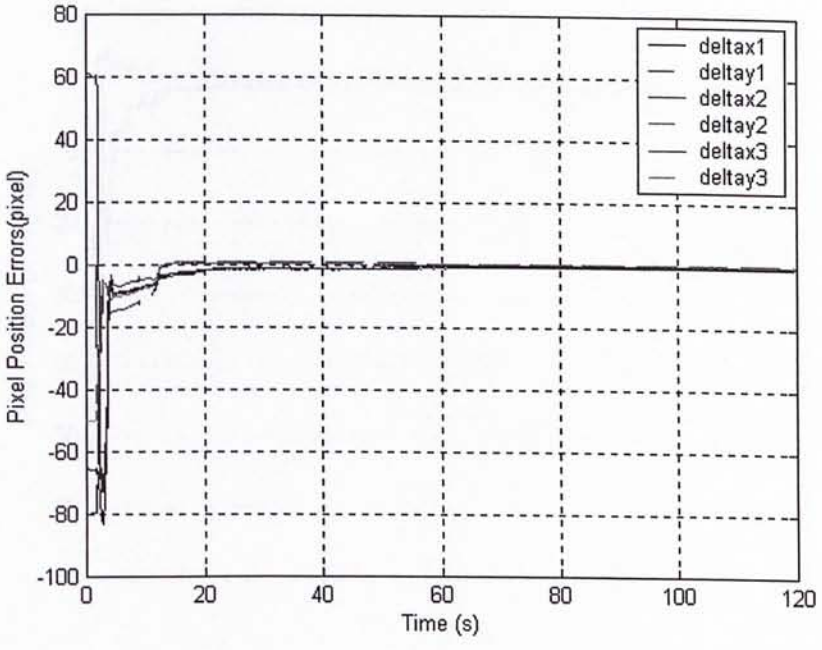

(a) Position errors of screen features

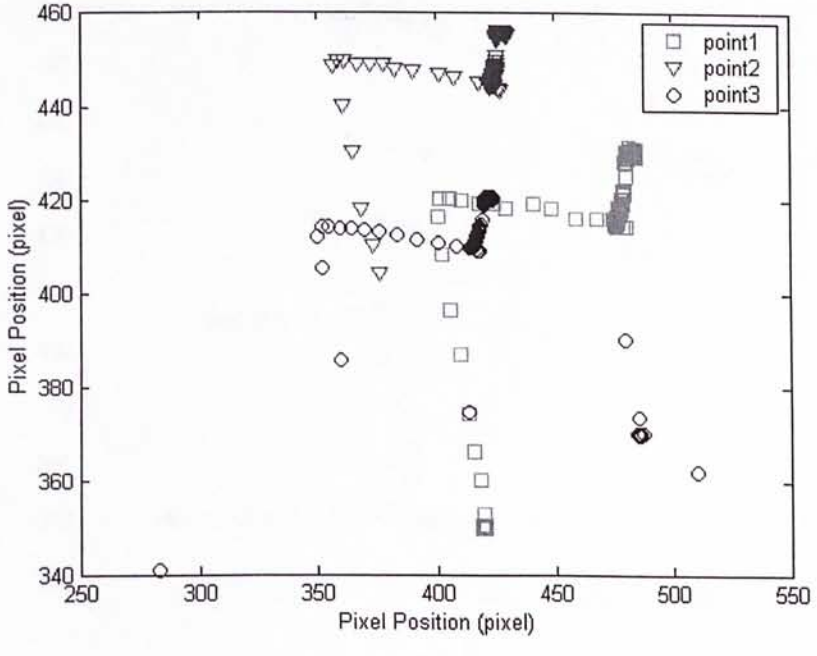

(b) Trajectories of screen features

Figure 5.4: The experimental result 1.

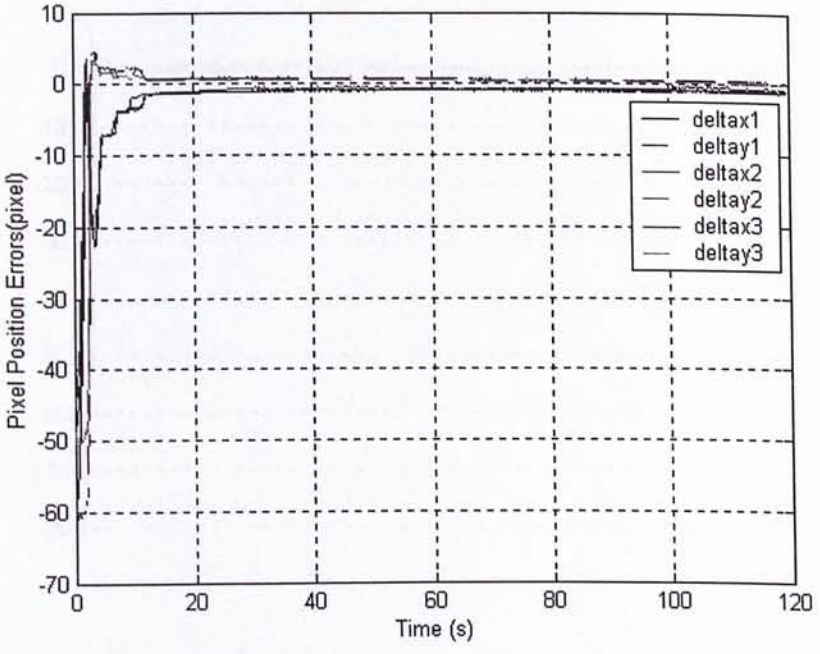

(a) Position errors of screen features

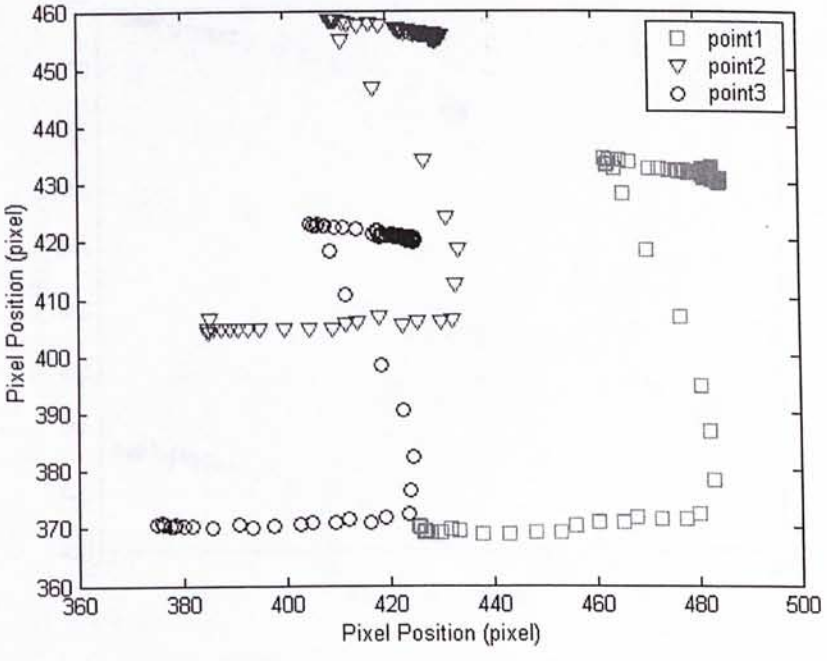

(b) Trajectories of screen features

Figure 5.5: The experimental result 2.

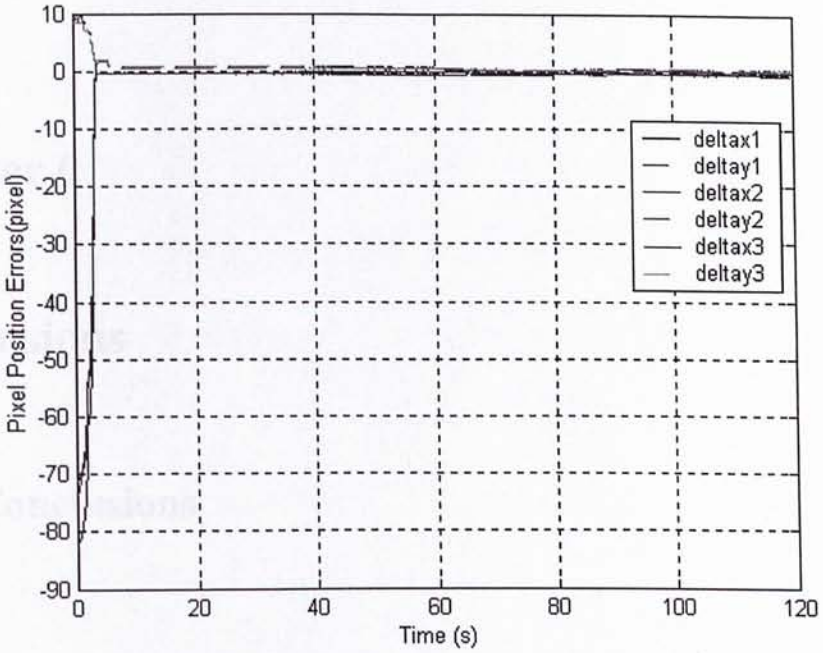

(a) Position errors of screen features

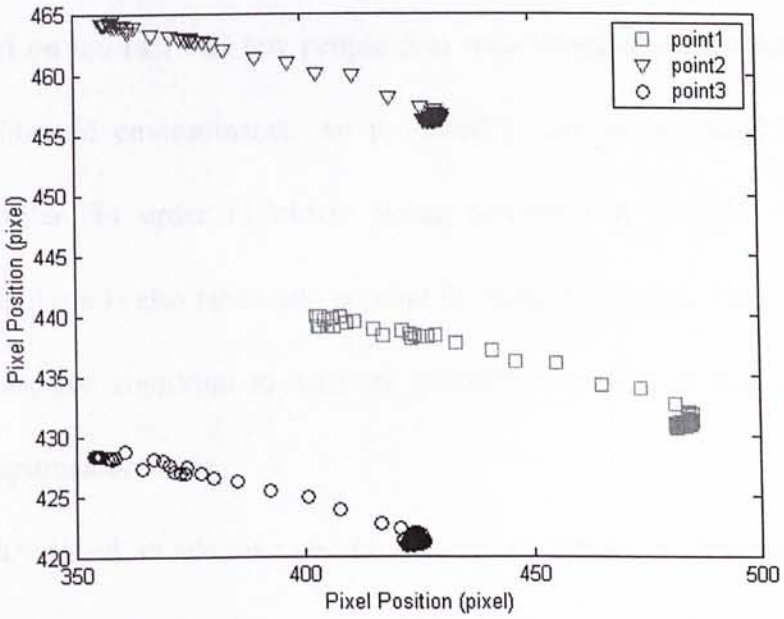

(b) Trajectories of screen features

Figure 5.6: The experimental result 3.

Chapter 6

Conclusions

6.1 Conclusions

In this thesis, we have studied the problems of uncalibrated visual servoing using an adaptive approach. The work of this thesis is summarized as follows:

(1) Based on the fact that few people deal with visual servo problems in totally uncalibrated environments, we proposed a new image-based visual servo controller. In order to obtain better performance, the full dynamics of manipulator is also taken into account in controller design. The controller uses an adaptive algorithm to estimate parameters on-line so that the system is asymptotically stable.

(2) We developed an adaptive law to estimate the unknown parameters including the camera intrinsic parameters and the homogeneous transformation matrix between the robot frame and the vision frame. The estimate parameters asymptotically approach to the actual ones up to a scale.

(3) We designed an image-based visual servo controller for an eye-and-hand system. It is proved with Lyapunov approach that the controller guarantees asymptotic convergence of the feature points errors on the image plane corresponding to the motion of the robot manipulator.

(4) The performance of the controller has been verified by computer simulations and experiments on a 3 DOF robot manipulator. The simulations and experiments results confirmed the expected convergence and high performance of the proposed controller.

6.2 Feature Work

In this thesis, we only conducted research on the regulation problem with uncalibrated visual feedback. Our feature work will be targeted on the following issues:

1. Uncalibrated trajectory tracking visual servo controller in image-based approach should be developed further.
2. The visual velocity is usually obtained by the distance over the period time. The sample rate is relative low in practice, which make the visual velocity measurement subject to big noises. We should develop a controller that uses only position instead of velocity.

3. This work is focused on eye-and-hand system. This control algorithm can also be applied to eye-in-hand systems. This should be developed further.

Appendix

A. Control Theory

We briefly review some control theories used to analyze stability of the systems in this thesis. These topics are covered in detail in book Slotine and Li [37], we only present some important results here.

Definition 1 (Stability)

The equilibrium state $x = 0$ is said to be stable if, for any R>0, there exists r>0, such that if $\|x(0)\| < r$, then $\|x(t)\| < R$ for all $t \geq 0$. Otherwise, the equilibrium point is unstable.

Definition 2 (Asymptotic Stability)

An equilibrium point 0 is asymptotically stable if it is stable, and if in addition there exists some $r > 0$ such that $\|x(0)\| < r$ implies that $x(t) \to 0$ as $t \to \infty$.

Definition 3 (Locally Positive Definite)

A scalar continuous function $V(x)$ is said to be locally positive definite if $V(0)=0$ and, in a ball B_{R_0}

$$x \neq 0 \Rightarrow V(x) > 0$$

if $V(0)=0$ and the above property holds over the whole state space, then $V(x)$ is said to be globally positive definite.

Definition 4 (Lyapunov Function)

If, in a ball B_{R_0}, the function $V(x)$ is positive definite and has continuous partial derivatives, and if its time derivative along any state trajectory of system $\dot{x} = f(x)$ is negative semi-definite, i.e.,

$$\dot{V}(x) \leq 0$$

then $V(x)$ is said to be a Lyapunov function for the system $\dot{x} = f(x)$

Theorem 1 (Local Stability)

If, in a ball B_{R_0}, there exists a scalar function $V(x)$ with continuous first partial derivatives such that

- $V(x)$ is positive definite (locally in B_{R_0})
- $\dot{V}(x)$ is negative semi-definite (locally in B_{R_0})

then the equilibrium point 0 is stable. If, actually, the derivative $\dot{V}(x)$ is locally negative definite in B_{R_0}, then the stability is asymptotic.

Theorem 2 (Global Stability)

Assume that there exists a scalar function V of the state x, with continuous first order derivatives such that

- $V(x)$ is positive definite
- $\dot{V}(x)$ is negative definite
- $V(x) \to \infty$ as $\|x\| \to \infty$

then the equilibrium at the origin is globally asymptotically stable.

Definition 5 (Invariant Set)

A set G is an invariant set for a dynamic system if every system trajectory which starts from a point in G remains in G for all future time.

Theorem 3(Global Invariant Set Theorem)

Consider the system $\dot{x} = f(x)$, with f continuous, and let $V(x)$ be a scalar function with continuous first partial derivatives. Assume that

- $V(x) \to \infty$ as $\|x\| \to \infty$

- $\dot{V}(x) \leq 0$ over the whole state space

let R be the set of all points where $\dot{V}(x) = 0$, and M be the largest invariant set in R.

then all solutions globally asymptotically converge to M as $t \to \infty$.

Theorem 4 (Barbalat's lemma)

If a scalar function $V(x,t)$ satisfies the following conditions

- $V(x,t)$ is lower bounded
- $\dot{V}(x,t)$ is negative semi-definite
- $\dot{V}(x,t)$ is uniformly continuous in time

then $\dot{V}(x,t) \to 0$ as $t \to \infty$.

Bibliography

[1] W. J. Wilson, C. C. W. Hulls, G. S. Bell, "Relative End-effector Control Using Cartesian Position Based Visual Servoing," *IEEE Trans. on Robotics and Automation,* Vol. 12, No. 5, pp.684-496, October 1996.

[2] E. Malis, F. Chaumette, S. Boudet, "Positioning a coarse-calibrated camera with respect to an unknown object by 2D 1/2 visual servoing," *Proc. Of the IEEE Int. Conf. on Robotics & Automation*, pp.1352-1359.1998.

[3] S. Hutchinson, G. D. Hager, and P. I. Corke, "A tutorial on visual servo control," IEEE Trans. Robot. Automat., vol. 12, pp.651-670, Oct. 1996.

[4] R. Kelly, R. Carelli, O. Nasisi, B. Kuchen, and F. Reyes, "Stable Visual Servoing of Camera-in-Hand Robotic Systems", *IEEE/ASME Trans. on Mechatronics*, Vol. 5, No.1, pp.39-48, March 2000.

[5] R. C. Luo, R. E. Mullen Jr., and D. E. Wessel, "An adaptive robotic tracking system using optical flow," in *Proc. IEEE Int. Conf. Robot. Automat.,* pp. 568-573, 1988.

[6] N. P. Papanikolopoulos and P. K. Khosla, "Adaptive Robotic Visual Tracking: Theory and Experiments," *IEEE Transaction on Automatic control*, Vol. 38, No. 3, pp. 429-445, 1993.

[7] K. Hosada and M. Asada, "Versatile Visual Servoing without knowledge of True Jacobain," *Proceedings of IEEE/RSJ International Conference on Intelligent Robots and Systems*, pp.186-191, 1994.

[8] B. H. Yoshimi and P. K. Allen, "Active, Uncalibrated Visual Servoing," *Proceedings of IEEE International Conference on Robotics and Automation*, pp. 156-161, 1994.

[9] J. T. Feddema and C. S. G. Lee, "adaptive image feature prediction and control

for visual tracking with a hand-eye coordinated camera" *IEEE Trans. On System, Man, amd Cybernetics*, 20(5):1172-1183, 1990.

[10] N. P. Papanikolopoulos, B. Nelson, and P. K. Khosla, "Six degree-of-freedom hand/eye visual tracking with uncertain parameters" *Proc. Of IEEE Int. Conf. On Robotics and Automation*, 174-179, 1994.

[11] R. Kelly, R. Carelli, O. Nasisi, B. Kuchen, and F. Reyes, "Stable visual servoing of camera-in-hand robotic systems," *IEEE/ASME Trans. Mechatron.*, vol. 5, pp. 39–48, Mar. 2000.

[12] R. Kelly and A. Marquez, "Fixed-Eye Direct Visual Feedback Control of Planar Robots", *J. Systems Engineering*, Vol. 4, No.5, pp. 239-248, Nov. 1995.

[13] R. Kelly, "Robust asymptotically stable visual servoing of planar robots," *IEEE Trans. Robot. Automat.*, vol. 12, pp. 759–766, Oct. 1996.

[14] E. Zergeroglu, D. M. Dawson, M. de Queiroz, and S. Nagarkatti, "Robust Visual-Servo Control of Planar Robot Manipulators in the Presence of Uncertainty", *Proc. of the 38th IEEE Conference on Decision and Control*, pp. 4137-4142, 1999.

[15] Maruyama, A. and Fujita, M, "Robust visual servo control for planar manipulators with the eye-in-hand configurations", *Proceedings of the 36th IEEE Conference on Decision and Control*, pp. 2551 – 2552, 1997.

[16] B.E. Bishop and M.W. Spong, "Adaptive Calibration and Control of 2D Monocular Visual Servo System", *IFAC Symp. Robot Control*, pp. 525-530, Nantes, France, 1997.

[17] R. Kelly, F. Reyes, J. Moreno, and S. Hutchinson, "A Two-Loops Direct Visual Control of Direct-Drive Planar Robots with Moving Target", *Proceedings of the IEEE International Conference on Robotics and Automation*, pp. 599-604, 1999.

[18] Piepmeier, J.A., McMurray, G.V. and Lipkin, H.," Tracking a moving target with model independent servoing: a predictive estimation approach", *Proc. IEEE ICRA*, pp2652-2657 , 1998.

[19] E. Zergeroglu, D.M. Dawson, M.S. de Queiroz, and A. Behal, "Vision-Based Nonlinear Tracking Controllers with Uncertain Robot-Camera Parameters",

Proceedings of the IEEE/ASME International Conference on Advanced Methatronics, pp. 854-859, 1999. Also accepted to appear in *IEEE/ASME Trans. On Mechatronics,* Vol. 6, No 3, September 2001.

[20] K. Hashimoto, T. Kimoto, T. Ebine, and H. Kimura, "Manipulator control with image-based visual servoing," in *Proc. IEEE Int. Conf. Robotics and Automation*, Sacramento, CA, 1991, pp. 2267–2272.

[21] Y. T. Shen, G. L. Xiang, Y. H. Liu and K. J. Li, "Uncalibrated Visual Servoing of Planar Robots," in *Proc. IEEE Int. Conf. Robotics and Automation*, pp.580-585, Washington, DC, May 2002.

[22] L. Hsu and P. L. S. Aquino, "Adaptive Visual tracking with Uncertain Manipulator Dynamics And Uncalibrated Camera", *Proceedings of the 38th IEEE Conference on Decision and Control*, pp.1248-1253, 1999.

[23] Ezio Malis, Fran¸cois Chaumette, and Sylvie Boudet, "2-1/2-D Visual Servoing", *IEEE Transaction on Robotics and Automation*, vol. 15, No. 2, 1999.

[24] Chaumette, F.; Malis, E., "2-1/2-D visual servoing: a possible solution to Improve image-based and position-based visual servoings", *IEEE International Conference on Robotics and Automation*, vol. 1, pp. 630 – 635, 2000.

[25] Cheah, C.C., Hirano, M., Kawamura, S. and Arimoto, S., "Approximate Jacobian Control With Task-Space Damping for Robot Manipulators", *IEEE Transactions on Automatic Control*, vol. 49(5), pp.752 – 757, 2004.

[26] Cheah, C.C., Hirano, M., Kawamura, S. and Arimoto, S., "Approximate Jacobian control for robots with uncertain kinematics and dynamics", *IEEE Transactions on Robotics and Automation*, vol. 19(4), pp. 692 – 702, 2003.

[27] C. J. Fang and S. K. Lin, "A performance criterion for the depth estimation with application to robot visual servo control", *Journal of Robotic System*, vol. 18, pp.609-622, 2001.

[28] F. Conticelli and B. Allotta, "Nonlinear controllability and stability analysis of adaptive image-based system", *IEEE Transaction on Robotics and Automation*, vol. 17, pp. 208-214, 2001.

[29] F. Conticelli, B. Allotta, and C. Colombo, "Hybrid visual servoing: A combination of nonlinear control and linear vision", *Robotics and Automation Systems*, vol. 29, pp.243-256, 1999.

[30] E. Malis, F. Chaumette, and S. Boudet, "2 1/2D visual servoing," *IEEE Trans. Robot. Automat.*, vol. 15, pp. 234–246, Apr. 1999.

[31] E. Malis and F. Chaumette, "2 1/2D visual servoing with respect to unknown objects through a new estimation scheme of camera displacement," *Int. J. Comput. Vis.*, vol. 37, no. 1, pp. 79–97, June 2000.

[32] L. Matthies and T. Kanade, "Kalman filter-based algorithms for estimating depth from image sequences", *Int. J. Computer Vision* vol. 3, pp.209-236, 1989.

[33] C.E. Smith, S.A. Brandt, and N.P. Papanikolopoulos, "Eye-in-hand robotic tasks in uncalibrated environments", *IEEE Transaction on Robotics and Automation,* vol.13 no. 6 pp.903-914, 1997.

[34] N. P. Papanikolopoulos, P. K. Khosla, "Adaptive Robotic Visual Tracking: Theory and Experiments," *IEEE Trans. on Automatic Control*, Vol. 38, No. 3, pp.429-445 , March 1993.

[35] R. Kelly and A. Coello, "Analysis and experimentation of transpose Jacobian based Cartesian regulators," *Robotica*, vol. 17, no. 3, pp. 303–312, May/June 1999.

[36] C. C. Cheah, S. Kawamura, and S. Arimoto, "Feedback control for robotic manipulators with an uncertain Jacobian matrix," *J. Robot. Syst.*, vol. 16, no. 2, pp. 119–134, 1999.

[37] J. J. E. Slotine and W. P. Li, "Applied Nonlinear control" 1991.

[38] D. A. Forsyth and J. Ponce, "Computer vision: a modern approach," Prentic Hall, 2003.